Formation of topological defects

from

symmetry-breaking phase transitions

in

Ion chains, Superconductors

&

Josephson Junctions

Lukas K. Brunkhorst

Supervisor: Emeritus Professor Raymond J. Rivers

Submitted in partial fulfilment of the requirements for the degree of
Master of Science in Theoretical Physics

12th September 2013

Department of Physics, Imperial College London

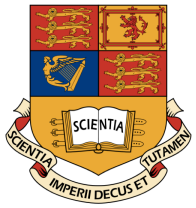

Contents

Introduction

Modern physics is formulated in a language that intensively employs the concept of symmetry in order to understand the fundamental phenomena encountered in nature. The notion of symmetry however soon becomes rather subtle. Often enough it is found to be realised in the ordinary sense – as an invariance of observables against a specified set of operations in *real* space. But in a further sense, symmetries may also be realised in the more abstract space of those quantities by which we aim to *describe* reality. In the second category fall situations in which even at the cost of redundancy, additional symmetries are created in order to obtain suitable mathematical descriptions. Complementary to what might be the intuiton, either approach proves not only successful in situations where the concerned symmetry is present, but rather becomes particularly valuable in its absence. The viewpoint suggested by the mathematical framework is that symmetries are never truly absent but under certain circumstances might merely be hidden. In fact, many of the most interesting phenomena in physics are observed on systems in such a state of hidden symmetry. Not the least, Grand Unified Theories understand three of the four fundamental interactions experienced in today's world as the remnants of what used to be unified in an early and more symmetric stage in the evolution of the universe. But the applicability of symmetry considerations is not constrained to the high energy scales. Only one prominent example being superconduction, a majority of the forms in which condensed matter appears can be understood in a similar way.

Whenever symmetry is being lost, this will be accompanied by the emergence of order and as such will become noticeable in the macroscopic appearance of a system. Transitions between states with different degrees of order are known as phase transitions and the standard framework in which to think of them is known by the name of spontaneous symmetry breaking. The thermodynamics of phase transitions are well understood and yield remarkable predictions, known as scaling and universality. In essence, these refer to the phenomenon that at their transitions, otherwise considerably different systems exhibit identical behaviour with respect to the relevant quantities and that the laws that describe this maintain their form at all different scales. Refined field-theoretic calculations could later made use of renormalisation group techniques to provide quantitative improvements to these scaling laws, while preserving their form. It were also renormalisation group ideas that finally led to an understanding of universality in terms of fixed points in the space of theories that is approached near phase transitions.

In contrast to the success in developing a consistent picture of equilibrium phase transitions, their non-equilibrium dynamics provide major obstacles to any attempt of a theoretical description. Apart from the limited validity of the thermodynamic limit,

the most important property of observable systems distinguishing them from idealised ones is that any process will be happening in a finite amount of time and it is this lack of adiabaticity which becomes crucial in the study of phase transitions. As will be illustrated in the course of this work, the formation of topological defects follows as an inevitable consequence of this and in fact all predictive power is largely constrained to a sensible description of these 'shards of broken symmetry' [1]. The investigation of their distribution spans a whole field of contemporary research, which has gained particular momentum by the ideas originating from Kibble and Zurek. While it is primarily not obvious if and why the thermodynamic results should be maintainable in non-equilibrium situation where phase transitions can be induced by strong external influences, the Kibble-Zurek mechanism provides an approximation scheme that succeeds to considerable extent in this respect. Its major achievement is to translate the equilibrium scaling laws into more general statements about the distribution of defects that has to be expected after a phase transition. Relying mainly on causality, the arguments invoked in this approach are of general applicability. While Kibble originally applied them in the context of predicting the formation of cosmic strings in the early universe, their recognition in condensed matter scenarios originates to Zurek, and since then there has been active collaboration between cosmologists and condensed matter physicists, hoping that each side could learn from the other. However, especially the tempting prospect of being able to draw conclusions about the structure of the universe from performing experiments in the laboratory has proven problematic. Reflected in the differences in structure towards the relativistic theories used in the cosmological setting, the inhomogeneities present in condensed matter put bounds on the presence of scaling in systems that are brought out of equilibrium.

The intention of this dissertation is to provide a broad, although therefore rather basic overview over the subject. A strong focus has been placed upon an extensive introduction to the elementary aspects of the underlying theory. In addition and exemplified by three of the experimental realisations currently enjoying the strongest interest, it is shown explicitly how their dynamics in the vicinity of a phase transition reflect the breaking of a symmetry and, supported by a numerical analysis, in how far the predictions of the Kibble-Zurek mechanism need to be extended.

Chapter 1 begins with a minimal review of the necessary concepts from thermodynamics and introduces the general notion of phase transitions in order to develop a further understanding based on the classic example of the ferromagnetic transition. The conceptual details of spontaneous symmetry breaking are elucidated and from the Landau approach to mean field theory, universality is motivated as a classification by critical exponents before a deeper explanation is given in terms of renormalisation. Chapter 2 shows which effects arise in non-equilibrium situations and how this gives rise to the production of topological defects. The Kibble-Zurek mechanism is presented as well as possible modifications to it in an elementary case. In chapter 3 all ideas are collected and found to be applicable to the three different realisations given in the title. Finally, the numerical simulations of defect formation in these systems are presented and evaluated in comparison to the predictions of Kibble and Zurek as well as more recent investigations. A summary concludes the work.

1. Theoretical Framework

Phase transitions are ubiquitous in nature. The fact that they can be observed in such a variety of different systems makes it difficult to describe the underlying physics in a general language without losing track of important details. Moreover, some mathematical subtleties will turn out to lie at the heart of critical behaviour. Hence it will be useful to always bear in mind a particular setting to refer to and for which the general ideas presented in the following can be made precise. This way, in turn, the general aspects to phase transitions will become much easier to appreciate. As the paradigmatic example for this cause the famous Ising model is chosen, which initially formed an attempt to explain ferromagnetism in the 1920s, but due to its phenomenological power today finds applications even in social network theory.

1.1 Basic Principles and Phenomenology

1.1.1 Thermodynamic basics

Statistical mechanics is the attempt to describe systems with a large number of degrees of freedom. In thermal equilibrium, this becomes a tractable task for which a systematic theoretical framework is available. A short account will be given here of those tools which will be most relevant for the present work. The main parts of the discussion, including notation, rely on [2].

Consider a physical system, represented in some abstract sample region Ω for which a Hamiltonian H_Ω can be defined. Further, assume that this region has a boundary $\partial\Omega$, and it is possible to define its volume $V(\Omega)$ and surface area $S(\Omega) = V(\partial\Omega)$. In the simplest case, Ω might be an ordinary cube with side length L. But even for more complicated geometries it is useful to think about the extent of a system approximately as

$$\begin{aligned} V(\Omega) &\propto L^d \\ S(\Omega) &\propto L^{d-1}, \end{aligned} \tag{1.1}$$

where d is the spatial dimensionality. A very basic question concerns the physical nature of the boundary. In principle, one could allow fluxes through $\partial\Omega$ and in fact this is what has implicitly been assumed in introducing a Hamiltonian and thus allowing for different energy levels in the system. If we excluded energy exchange with the surroundings, i.e. if we were examining a perfectly isolated system, we could simply replace H_Ω by a definite energy E. On the other hand, we do not wish to be concerned about an exchange of particles through $\partial\Omega$, as would be necessary for

membrane-like surfaces. The resulting picture is the one referred to as *canonical ensemble*. The Hamiltonian can be written in terms of the coupling constants $\{K_n\}$ and combinations of the $N(\Omega)$ dynamical degrees of freedom $\{\Theta_n\}$ as

$$H_\Omega = -\frac{1}{\beta}\sum_n K_n \Theta_n, \tag{1.2}$$

where, introducing Boltzmann's constant k_B, $1/\beta = k_B T$ defines a basic thermal energy scale which is determined by the temperature T. The temperature is itself part of the set $\{K_n\}$ that also contains other external parameters such as present fields.

The central object that can be computed from this stage is the *partition function*

$$Z[\{K_n\}] = \mathrm{Tr}\, \mathrm{e}^{-\beta H_\Omega}\,. \tag{1.3}$$

Taking the trace here means summing over all configurations of the system,

$$\mathrm{Tr} = \sum_{\Theta_1}\sum_{\Theta_2}...\sum_{\Theta_{N(\Omega)}}\,, \tag{1.4}$$

each one weighted by the Boltzmann factor $e^{-\beta H_\Omega}$ evaluated at the respective values of the external parameters. The meaning of this factor is that in thermal equilibrium the probability of measuring the system to be in a state of energy E is

$$p(E) = \frac{\mathrm{e}^{-\beta E}}{Z}\,. \tag{1.5}$$

A good derivation of this result can be found in [3].

The significance of the partition function is that all thermodynamic properties of Ω are encoded in it. Or to be precise, they are the derivatives of the *free energy* with respect to the coupling constants, where the free energy is defined as

$$F_\Omega[\{K_n\}] = -\frac{1}{\beta}\log Z_\Omega\,. \tag{1.6}$$

There is also a second, equivalent expression for the free energy that relies on a definition of entropy. The relation between the two forms is quickly revealed:
First consider the average internal energy

$$U := \sum_r E_r p(E_r) = -\frac{\partial}{\partial\beta}\log Z \tag{1.7}$$

as well as the generalised forces

$$\kappa_{n|r} = -\frac{\partial E_r}{\partial K_n}\,, \tag{1.8}$$

with averages

$$\kappa_n := \sum_r p(E_r)\kappa_{n|r} = \frac{1}{\beta}\frac{\partial \log Z}{\partial K_n}\,. \tag{1.9}$$

We can then write

$$\begin{aligned} \mathrm{d}\log Z &= \frac{\partial \log Z}{\partial \beta}\,\mathrm{d}\beta + \sum_n \frac{\partial \log Z}{\partial K_n}\,\mathrm{d}K_n \\ &= -U\mathrm{d}\beta + \beta \sum_n \kappa_n\,\mathrm{d}K_n \\ &= -\mathrm{d}(\beta U) + \beta\,\mathrm{d}U + \beta \sum_n \kappa_n\,\mathrm{d}K_n\,. \end{aligned} \tag{1.10}$$

The second law of thermodynamics reads

$$\mathrm{d}U = T\mathrm{d}S - \sum_n \kappa_n \mathrm{d}K_n\,, \tag{1.11}$$

with the entropy defined as

$$S = k_B \log \omega \tag{1.12}$$

where ω denotes the number of microstates compatible with a certain macroscopic state of Ω. Combining eqn. (1.10) and (1.11) to

$$S = \int_{T=0} \mathrm{d}S = \frac{U}{T} + k_B \log Z\,, \tag{1.13}$$

we can conclude that

$$F_\Omega = U - TS \tag{1.14}$$

is the free energy from above in eqn. (1.6), but as a function of the entropy S. The integration constant in eq. (1.13) has been omitted as it can be determined to be zero from looking at the limit $\lim_{T\to\infty} S$.

Finally, we have to invoke the *thermodynamic limit*, which is usually defined as the limiting procedure

$$\begin{aligned} &N(\Omega) \to \infty \quad \text{and} \quad V(\Omega) \to \infty \\ &\qquad \text{s.t.} \quad \frac{N(\Omega)}{V(\Omega)} = \text{const.} \end{aligned} \tag{1.15}$$

and without which phase transitions have no formally precise meaning, as will become clear later. In this limit the free energy also becomes infinite – it is extensive. Two better, that is, *intensive* quantities to work with in the thermodynamic limit are the associated bulk and surface densities

$$\begin{aligned} f_b &= \lim_{V(\Omega)\to\infty} \frac{F_\Omega[\{K_n\}]}{V(\Omega)} \\ f_s &= \lim_{S(\Omega)\to\infty} \frac{F_\Omega[\{K_n\}] - V(\Omega) f_b}{V(\Omega)}\,. \end{aligned} \tag{1.16}$$

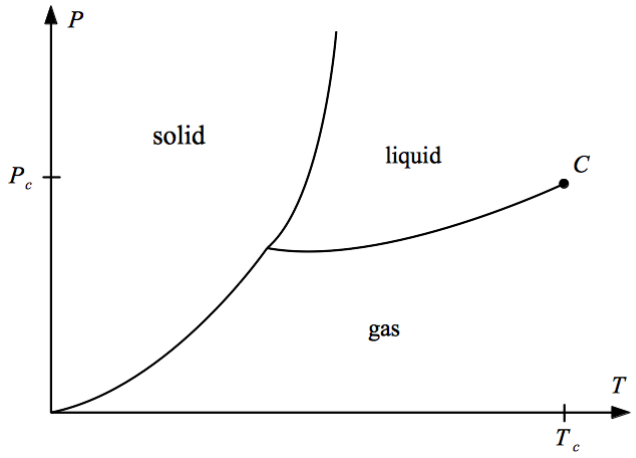

Figure 1.1: Schematic form of a typical temperature-pressure phase diagram. A continuous phase transition happens only at the critical point C.

For systems defined on a lattice the quantity that corresponds to f_b and which we will use extensively is the free energy per degree of freedom

$$f = \lim_{N(\Omega)\to\infty} \frac{F_\Omega[\{K_n\}]}{N(\Omega)} \tag{1.17}$$

It is important to note however that there are cases in which the thermodynamic limit does not exist. One example for which f_b diverges in the limit is a uniform cloud of equally charged particles [2].

1.1.2 Classification of phase transitions

The fact that the same matter can develop very different macroscopic appearance depending on the external circumstances and the observation of transitions between the different states calls for a systematic classification. A pictorial way to capture this type of phenomena is given by phase diagrams like in fig. 1.1.2, where the parameter space is partitioned into regions of equal phase, seperated from each other by phase boundaries.

Mathematically, phase boundaries are identified as sets of points in parameter space where certain thermodynamic functions become singular. This is only possible in the thermodynamic limit since for finite systems the partition function must always be the sum of analytic functions and thus can never exhibit singularities. An infinite number of terms however can produce discontinuities or infinities at certain parameter values. Because usually observed systems have a large number of degrees of freedom ($\sim 10^{23}$) sharp phase transitions will never appear in any experiment but instead the phase boundaries are observed to be smeared out.

When Ehrenfest developed the original classification scheme, he distinguished between phase transitions of *first* and *second order*. While in the former case the first

derivative of the thermodynamic potential with respect to the relevant parameter exhibits a discontinuity at the critical point, in the latter case it is the second. In the modern approach phase transitions are characterised by whether or not latent heat is developed. The advantage of this criterion is that it is accessible to experiment. At the same time, it generalises Ehrenfest's scheme, which is why it is usually preferred today. Transitions which are accompanied by latent heat are referred to as *discontinuous*, and would have been identified as of first order by Ehrenfest. One familiar example of a discontinuous phase transition is the boiling of water. The change of phase from liquid to vapour does not happen instantaneously but gradually throughout the system and in order to maintain the process thermal energy has to supplied by the environment. Phase transitions that occur without latent heat are called *continuous*, and fall into the second order category. These processes are usually realised only in distinct regions of parameter space, labelled as *critical points* (or surfaces). The non-analytic behaviour of systems undergoing continuous phase transitions displays an extraordinary richness and is summarised under the name of *critical phenomena*. Instances of these provide the foundation of this work.

From comparison in terminology between the two classification schemes, it is evident that from the modern point of view only the first derivative of the thermodynamic potential plays a distinct role. Although rare, discontinuities in higher than second derivatives are not excluded and all fall into the same class of continuous phase transitions.

In order to quantify the meaning of a phase, it is appropriate to define an observable that takes on distinct values in the different phases and thus makes them distinguishable. Such a quantity is called an *order parameter* and its choice is not necessarily unique. The common definition is, that it only needs to be zero in one phase and non-zero but finite in the other. However, there are deviations from this rule, as will be seen in sec. 1.1.3 for the zero-temperature transition in the Ising model. The term 'order parameter' itself originates from the fact that, as will be seen, phase transitions can be understood as the breakdown of some degree of order in a system. Nevertheless, order parameters can also be defined more abstractly, independent of this meaning.

So far, the discussion was concerned with classical phase transitions, which are driven by thermal fluctuations. At low temperatures however, quantum fluctuations become relevant, spanning a whole new field of analysis. In fact, at $T = 0$ it is possible to define quantum phases and again there exist transitions between these, with a separate range of effects. However, this will not be treated.

1.1.3 Ising model

All materials react on an externally applied magnetic field $\mathbf{H}$ by exhibiting a magnetisation $\mathbf{M}$, resulting in a magnetostatic force. For pure diamagnets this force is repulsive and often negligible, while for paramagnets it becomes attractive but, with some exceptions, also stays small so that in both cases and for large temperature ranges the magnetisation can be seen as a *linear response* to the magnetic field as long as this does not exceed a certain critical strength. In contrast, when cooled down below a material-specific temperature, *ferromagnets* are capable of exhibiting a large magnetisation even without an externally applied magnetic field. It was this phe-

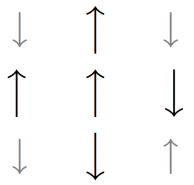

Figure 1.2: A representative 3×3 block of a two-dimensional Ising lattice in some random configuration at a single instant in time. Only nearest neighbours interact in the Ising model, here represented by bigger arrows.

nomenon that Lenz and Ising aimed to understand when they established the Ising model during the years from 1920 to 1925. With the Stern-Gerlach experiment performed in 1922, a rigorous theory of spin was only at its start. But already had it been understood that there exists a two-valued internal degree of freedom attributable to atoms with unpaired electrons, giving rise to microscopic magnetic dipoles. The Ising model formalises this observation by considering $N(\Omega)$ interacting spins on a lattice of which we label the vertices by an index i. To each lattice site a variable is assigned that has only two possible values

$$S_i = \pm 1 \qquad \forall\ i = 1 \dots N(\Omega)\,, \tag{1.18}$$

corresponding to the spin being either up or down. The crucial simplification is to restrict the interaction between spins only to nearest neighbours. Even bearing in mind the rapid, inversely cubic radial fall-off in magnitude of the magnetic dipole interaction, this assumption seems like an oversimplification at first sight but will turn out to yield major insights already. Is is the power of the Ising model that it replaces the complicated quantum mechanical interaction between the lattice constituents by an almost trivial-seeming term while retaining a great amount of predictive strength. This is in fact a first example of a more general phenomenon which will be adressed later in this work. This section will be restricted to the discussion of a lattice with hypercubic structure, the lattice spacing being denoted as a. As for now, we can leave the spatial dimension d unspecified. The Ising Hamiltonian in its simplest form assumes a uniform magnetic field and equal coupling between all pairs of neighbouring spins – denoted by $\widehat{ij}$ – and can be written as

$$H_\Omega = -H \sum_{i=1}^{N(\Omega)} S_i - J \sum_{\widehat{ij}} S_i S_j\,. \tag{1.19}$$

This is readily justified phenomenologically: Pointing in the direction of the magnetic field and aligning with the nearest neighbours is energetically favourable for each single spin (assuming $J > 0$). The ground state will thus be

$$S_i = \begin{cases} +1 & \text{for } H > 0 \\ -1 & \text{for } H < 0 \end{cases} \qquad \forall i \quad (J > 0)\,. \tag{1.20}$$

We will now see that this is the first instance of a phase transition we encounter. The corresponding order parameter is the magnetisation

$$M_\Omega := \frac{1}{N(\Omega)} \sum_i S_i \,, \tag{1.21}$$

which is nothing but the normalised first derivative of the free energy (1.14) with respect to the external field H,

$$M_\Omega = -\frac{1}{N(\Omega)} \frac{\partial F_\Omega}{\partial H} = -\frac{\partial f}{\partial H} \,, \tag{1.22}$$

for free energy density f. At $T = 0$, the value of M_Ω changes from $+1$ for $H > 0$ towards -1 for $H < 0$, so it has indeed the correct bahaviour for an order parameter as introduced in sec. 1.1.2. For $H = 0$ however, the two states of all spins up and all spins down are energetically degenerate and we cannot make a statement about the expected value of M_Ω. In fact, which value M_Ω assumes will depend on nothing but the initial conditions on the system. We will return to this point later, when discussing spontaneous symmetry breaking. For now, let us relax the condition of zero temperature to make the discussion more generally applicable. For non-zero temperature $T > 0$, each of the $N(\Omega)$ spin degrees of freedom carries kinetic energy, approaching $k_B T/2$ for increasing T as stated by the equipartition theorem. Correspondingly, a finite entropy is emerging and the spin system will tend to minimise the free energy instead of only the internal energy. As shown in section 1.1.1, the free energy density f is derived from the partition function, which for the Ising model takes the form

$$Z_\Omega = \sum_{\{S_i = \pm 1\}} \mathrm{e}^{-\beta H_\Omega(\{S_i\})} \,. \tag{1.23}$$

Here we have partly abandoned notational rigour and only made explicit the dependence of the Hamiltonian (1.19) on the configuration of spins. One important symmetry of the Ising model can be identified at this point. Regarding eqn. (1.23), one realises that because Z_Ω is evaluating a configuration-dependent function and sums over *all* possible configurations every term has a partner term corresponding to the same configuration but with all spins flipped. Thus the whole sum is invariant against a simultaneous change of sign in all spin variables S_i

$$\mathbb{Z}_2 : \quad S_i \to -S_i \quad \forall i \tag{1.24}$$

where the associated symmetry group has been recognised as the smallest discrete group, that is $\mathbb{Z}_2$. The Hamiltonian transforms under its action as

$$\begin{aligned} H_\Omega(H, J, \{S_i\}) \quad &\longrightarrow \quad H_\Omega(H, J, \{-S_i\}) \\ &= H_\Omega(-H, J, \{S_i\}) \,. \end{aligned} \tag{1.25}$$

It follows that the free energy density is even in the magnetic field H:

$$f(H, J, T) = f(-H, J, T) \tag{1.26}$$

We could also try and reverse only single spins instead of all spins at once. An operation of this kind still leaves the value of Z_Ω unaltered but clearly changes H_Ω,

the energy of a configuration. That is why we refer to the $\mathbb{Z}_2$ symmetry of the Ising model as being *global* (or rigid) as opposed to local. It can also be understood as a *time reversal* symmetry when the spin is being associated with the direction of the magnetic moment arising from an electronic current at atomic level.

Let us now ask for the physical relevance of this global $\mathbb{Z}_2$ in the Ising model. The central question is in how far this symmetry property will become visible not only in the equations that describe the system, but also in its actually realised states.

When discussing the form of the Hamiltonian (1.19) a partial answer to this was already found. The ground state at $T = 0$ was seen to be a configuration of all parallel spins — a state clearly not symmetric under the $\mathbb{Z}_2$ action above. For high temperatures on the other hand, thermal fluctuations become dominant and at $H = 0$ the states can be regarded as $\mathbb{Z}_2$-symmetric as long as we average over short time (or length) scales with the magnetisation being zero. The exact argument is slightly more subtle and will be presented in detail later. But accepting this, then it has to be expected that, when lowering the temperature, from some distinct temperature on it will become favourable again for the system to regain some of the long range order exhibted in its ground state. This is indeed what happens and the mathematical picture that captures this symmetry breaking process for a general setting is being elucidated in sec. 1.1.4. For now, the aim is to explore in some more detail the Ising model as a representative system.

We start with one single spatial dimension, $d = 1$, and ask how thermal fluctuations in general influence the ground state at $H = 0$. To answer this, we first examine one of the two $T = 0$ ground states, say the one with all N spins up:

$$... \uparrow\uparrow\uparrow\uparrow\uparrow\uparrow\uparrow\uparrow ...$$

The free energy of this state is simply

$$F_N = -NJ\,. \tag{1.27}$$

If thermal energies are high enough to flip a finite fraction of spins, a positive contribution to the entropy is to be expected. It is worth noting that for this to be true in the thermodynamic limit, an infinite number of reversals would be needed. It is thus much more convenient to speak about regions of spins with the same orientiation rather than about that of each spin separately. Regions of uniform microscopic configuration like this are generally referred to as *domains*. What marks the transtion between two domains is called a *domain wall*, or *defect*. In the groundstate from above there is only one single domain. Adding one domain or, equivalently, inserting one defect, the microscopic state looks like

$$... \uparrow\uparrow\uparrow\uparrow ... \uparrow\uparrow\downarrow\downarrow ... \downarrow\downarrow\downarrow\downarrow ... \tag{1.28}$$

or like its mirror image. The change of orientation from one to the other side of the domain wall has cost an energy of $\Delta E = +2J$, no matter where in the chain the defect sits. For perdiodic boundary conditions, the entropy of the state is thus

$$S_N = k_B \log N\,, \tag{1.29}$$

whereas in the case of open ends, $S_N = k_B \log(N-2)$, which for large N does not make a considerable difference. Assuming the periodic case, the difference in free

energy to the ground state becomes

$$\Delta F_N = 2J - k_B T \log N \tag{1.30}$$

which is negative for all temperatures $T > 2J/k_B \log N$. But from $\Delta F_N < 0$ we conclude that all the states with one defect are now thermodynamically preferred by the system. In fact, in the limit $N \to \infty$, defect creation becomes preferrable for *any* temperature, $\Delta F_N \to -\infty \ \ \forall\ T > 0$. By repeatedly applying the above argument to the domains, it becomes obvious that for $T > 0$ the configuration of lowest free energy will have no domains left:

$$... \uparrow\downarrow\uparrow\downarrow\uparrow\downarrow\uparrow ... \tag{1.31}$$

While for $T = 0$ the magnetisation was either $+1$ or -1, now it is strictly zero. This also means that the phase transtion occuring when H changes sign vanishes for non-zero temperatures. This is because the long range order encoded in the nearest-neighbour spin interaction is unstable against even the smallest thermal fluctuations. There are simply no more two different possible phases existent at $H = 0$.

The result, that the Ising model in $d = 1$ lacks a finite temperature phase transitions, explicitly relies on the nature of the assumed interaction in the model. However, there is a generalisation to this. Promoting the interaction strength J to a function of the distance r between lattice sites, $J \to J(r)$, it was established [4] that in fact there *do* exist phase transitions for sufficiently long-ranged interaction. Assuming the form

$$J(r) \propto \frac{1}{r^\alpha} \tag{1.32}$$

this is precisely the case for $1 \leq \alpha \leq 2$, while for $\alpha > 2$ the interaction qualifies as being short-ranged.

Increasing the number of space dimensions d, the number of nearest neighbours for each lattice site will increase. Consequently, not only for the Ising model but quite generically, the effect of internal interactions on the free energy will rise compared to the remaining, externally caused energetic contributions. This means that long range order is more likely to be seen in higher values of d. If a model does not exhibit a $T \neq 0$ phase transition in some low space dimension, it might still do so in higher dimensions. If this is the case, a *lower critical dimension* d_c can be identified, which marks the maximal space-dimensionality at which the interactions are just not strong enough to give rise to long-range order. For the Ising model, $d_c = 1$. This means that mathematically, the model exhibits a transitions for any $d = d_c + \epsilon$ with $\epsilon > 0$ as can be shown by a more rigorous analysis. We shall subsequently only give the phenomenological reasoning for the next integer dimension.

In two space dimensions, the energy difference between a state with all spins pointing in the same direction and one exhibiting a domain wall along $\hat{n}$ lattice sites will be of the order

$$\Delta E \simeq 2J\hat{n}\,. \tag{1.33}$$

The entropy of the state with one domain now becomes more difficult to calculate than in $d = 1$. As a first approximation however, we can make the analogy to a

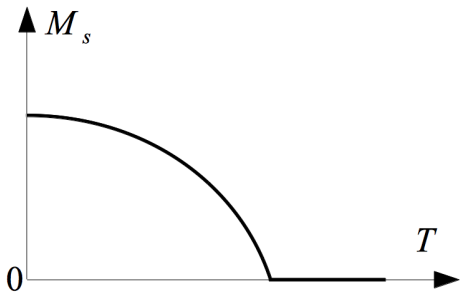

Figure 1.3: Spontaneous magnetisation $M_s \equiv \pm \lim_{H \to 0^\pm} \partial f / \partial H$ as a function of temperature. That fact that it is continuous indicates that the ferromagnetic phase transition is of second order.

random walk. If the co-ordination number of our lattice is z, i.e. each lattice site has z nearest neighbours, then there will be roughly $(z-1)^n$ possible shapes the domain wall can take, because it cannot intersect itself in the state of only one domain. This guess will be an overestimate, because we have neglected the existence of boundaries. The corresponding entropy is

$$\Delta S \simeq k_B \hat{n} \log(z-1) \tag{1.34}$$

and so the change in free energy will be

$$\Delta F \simeq \hat{n}(2J - k_B T \log(z-1)) \,. \tag{1.35}$$

As before, we require $\hat{n}$ to be a non-zero fraction of N so that $\hat{n} \to \infty$ in the thermodynamic limit. Then we can identify a critical temperature at which ΔF changes sign and thus distinguishes between $\Delta F \to +\infty$ and $\Delta F \to -\infty$ in the thermodynamic limit. This *critical temperature* is

$$T_c \simeq \frac{2J}{k_B \log(z-1)} \,. \tag{1.36}$$

It is not surprising that T_c depends on the shape of the lattice. Denser lattices (higher z) are less susceptible to long range order. However, unlike the space dimensionality d, it only affects *when* the transition occurs, and not *if* it occurs.

As in the case of $d = 1$ the argument above can be extended to states with more than one domain wall and so we conclude that T_c separates two phases. For higher temperatures $T > T_c$, the system becomes unstable against thermal fluctuations, domains vanish, and the magnetisation will be strictly zero. For lower temperatures $T < T_c$, long-range order is protected against thermal effects and the magnetisation will be finite, either positive or negative. It will continue to increase with decreasing temperature until it reaches its maximum absolute value $|M| = 1$ at $T = 0$. The exact behaviour can be calculated and is shown in fig. 1.1.3.

The arguments presented in this chapter are not only applicable to a $\mathbb{Z}_2$ symmetric system like the Ising model. Similar reasoning stays valid also in systems invariant

under *any* discrete symmetry group. The fact that these properties were derived from a $\mathbb{Z}_2$ symmetric system but are extendable to situations exhibiting other symmetries supports the approach of F. Baroni, who promotes this observation to the conjecture that actually all of what is necessary to understand phase transitions might be seen from $\mathbb{Z}_2$ symmetric models [5].

Up to now we have only given semi-phenomenological arguments. To complete the discussion, the actual formal solution to the $d = 1$ Ising model will be presented, most importantly because it employs the transfer matrix technique, which is of wide applicability in statistical physics. The difficult two-dimensional case was solved exactly by Onsager [6] whereas no analytical solution is known for higher dimensions.

Writing out the $d = 1$ partition function (1.23) by using the Hamiltonian (1.19) gives, when simplifying notation to $N \equiv N(\Omega)$ and assuming periodic boundary conditions $S_{N+1} = S_1$ for convenience,

$$Z_\Omega = \sum_{\{S_i=\pm 1\}} \prod_{j=1}^{N} \exp\Big\{\beta\Big[\frac{1}{2}H\,(S_j + S_{j+1}) + J\,S_j S_{j+1}\Big]\Big\} \tag{1.37}$$

The surprising observation is that this can be written as a trace, and a reader familiar with quantum mechanics and the density matrix formulation will notice the close formal analogy. Defining the 2×2 *transfer matrix* T to have components

$$T_{S_i S_j} = \exp\Big\{\beta\Big[\frac{1}{2}H\,(S_j + S_{j+1}) + J\,S_j S_{j+1}\Big]\Big\}, \tag{1.38}$$

implies its matrix form to be

$$T = \begin{pmatrix} \mathrm{e}^{\beta(H+J)} & \mathrm{e}^{-\beta J} \\ \mathrm{e}^{-\beta J} & \mathrm{e}^{\beta(-H+J)} \end{pmatrix} \tag{1.39}$$

and the partition function becomes

$$Z_\Omega = \mathrm{Tr}\left(T^N\right). \tag{1.40}$$

The trace operation is invariant against a change of basis, and so we diagonalise into the eigenbasis of T to realise that

$$Z_\Omega = \lambda_+^N + \lambda_-^N \tag{1.41}$$

with eigenvalues

$$\begin{aligned} \lambda_\pm &= \frac{\mathrm{Tr}\,T}{2} \pm \sqrt{\Big(\frac{\mathrm{Tr}\,T}{2}\Big)^2 - \det T} \\ &= \mathrm{e}^{\beta J}\cosh\beta H \pm \sqrt{\mathrm{e}^{2\beta J}\sinh^2\beta H + \mathrm{e}^{-2\beta J}}\,. \end{aligned} \tag{1.42}$$

The free energy density then becomes

$$f = -k_B T \ln\left(\lambda_+^N + \lambda_-^N\right). \tag{1.43}$$

Note that in the thermodynamic limit the contribution from the smaller eigenvalue λ_- becomes neglible and $Z_-\Omega \to \lambda_+^N$ so that the system's behaviour remains completely

determined by the largest eigenvalue of the transfer matrix. Having obtained an analytic expression for the partition function, we could simply invoke the canonical derivative formulas to calculate the magnetisation or any other observable. In this case however, it is easier to further employ the transfer matrix method.

Still maintaining periodic boundary conditions, we conclude for the magnetisation,

$$\begin{aligned} M_\Omega &= \langle S_j \rangle \\ &= \frac{1}{Z_\Omega} \sum_{\{S_i=\pm 1\}} T_{S_1 S_2} \dots T_{S_{j-1} S_j} S_j T_{S_j S_{j+1}} \dots T_{S_N S_1} \\ &= \frac{\mathrm{Tr}\big(T^j \sigma_z T^{N-j}\big)}{\lambda_+^N + \lambda_-^N} = \frac{\mathrm{Tr}\big(\sigma_z T^N\big)}{\lambda_+^N + \lambda_-^N} \,, \end{aligned} \tag{1.44}$$

where the third Pauli matrix σ_z was introduced. T is real and symmetric, so that there exist an orthogonal transformation matrix R ($R^t = R^{-1}$) that diagonalises T. Using the second Pauli matrix σ_y, we parametrise the rotation as $R(\theta) = \exp(i\theta\sigma_y)$ by an angle θ that can be read off from eqn. (1.39) to obey

$$\begin{aligned} \tan 2\theta &= \sqrt{\frac{\mathrm{e}^{-2\beta J}}{\mathrm{e}^{2\beta J} \sinh^2 \beta H}} \\ &= \mathrm{e}^{-2\beta J} \sinh^{-1} \beta H \,. \end{aligned} \tag{1.45}$$

Hence,

$$T \longrightarrow R(\theta)\, T\, R^t(\theta) = \begin{pmatrix} \lambda_+ & 0 \\ 0 & \lambda_- \end{pmatrix} =: \Lambda \,. \tag{1.46}$$

The implicit use of this in eqn. (1.44) led to the simple form of Z. Now however, introducing $R(\theta)$ explicitly was necessary as we are left with

$$\begin{aligned} M_\Omega &= \frac{\mathrm{Tr}\big(\sigma_z [R^t(\theta)\, \Lambda\, R(\theta)]^N\big)}{\lambda_+^N + \lambda_-^N} = \frac{\mathrm{Tr}\big(\sigma_z R^t(\theta)\, \Lambda^N R(\theta)\big)}{\lambda_+^N + \lambda_-^N} \\ &= \frac{\mathrm{Tr}\big(R(\theta) \sigma_z R^t(\theta)\, T^N\big)}{\lambda_+^N + \lambda_-^N} \,. \end{aligned} \tag{1.47}$$

We compute

$$\begin{aligned} R(\theta)\sigma_z R^t(\theta) &= \exp(i\theta\sigma_y)\sigma_z \exp(-i\theta\sigma_y) \\ &= \begin{pmatrix} \cos\theta & \sin\theta \\ -\sin\theta & \cos\theta \end{pmatrix} \begin{pmatrix} 1 & 0 \\ 0 & -1 \end{pmatrix} \begin{pmatrix} \cos\theta & -\sin\theta \\ \sin\theta & \cos\theta \end{pmatrix} \\ &= \begin{pmatrix} \cos 2\theta & -\sin 2\theta \\ -\sin 2\theta & -\cos 2\theta \end{pmatrix} \end{aligned} \tag{1.48}$$

to find the result for the magnetisation:

$$M_\Omega = \frac{\lambda_+^N - \lambda_-^N}{\lambda_+^N + \lambda_-^N} \cos 2\theta \tag{1.49}$$

Again, the contribution of λ_- vanishes in the thermodynamic limit, where $M_\Omega \to \cos 2\theta$. Note also that M_Ω does not depend on j, as it should be.

A measure for spin fluctuations is given by the connected two-point correlation function

$$\begin{aligned} G_{ij} &:= \langle S_i S_j \rangle - \langle S_i \rangle \langle S_j \rangle \\ &= \langle S_i S_j \rangle - M_\Omega^2 \end{aligned} \tag{1.50}$$

Periodic boundary conditions encode translational invariance via the trace, and so correlations can only depend on the difference $i - j$. We calculate:

$$\begin{aligned} &\langle S_i S_{i+j} \rangle = \langle S_1 S_j + 1 \rangle \\ &= \frac{1}{Z} \mathrm{Tr}\big(\sigma_z T^j \sigma_z T^{N-j}\big) = \frac{1}{Z} \mathrm{Tr}\Big[R(\theta)\sigma_z R^t(\theta) \Lambda^j R(\theta) \sigma_z R^t(\theta) \Lambda^{N-j}\Big] \\ &= \frac{1}{\lambda_+^N - \lambda_-^N} \mathrm{Tr}\left[\begin{pmatrix} \lambda_+^j \cos 2\theta & -\lambda_-^j \sin 2\theta \\ -\lambda_+^j \sin 2\theta & -\lambda_-^j \cos 2\theta \end{pmatrix} \begin{pmatrix} \lambda_+^{N-j} \cos 2\theta & -\lambda_-^{N-j} \sin 2\theta \\ -\lambda_+^{N-j} \sin 2\theta & -\lambda_-^{N-j} \cos 2\theta \end{pmatrix} \right] \\ &= \frac{1}{\lambda_+^N - \lambda_-^N} \Big[\cos^2 2\theta \left(\lambda_+^N + \lambda_-^N\right) + \sin^2 2\theta \left(\lambda_+^{N-j} \lambda_-^j + \lambda_-^{N-j} \lambda_+^j\right) \Big] . \end{aligned} \tag{1.51}$$

Here,

$$\langle S_i S_{i+j} \rangle \;\longrightarrow\; \cos^2 2\theta + \left(\frac{\lambda_-}{\lambda_+}\right)^j \sin^2 2\theta \qquad \text{for} \quad N \to \infty \tag{1.52}$$

and we conclude for correlations in the thermodynamic limit:

$$G_{ij} = \sin^2 2\theta \Big(\frac{\lambda_-}{\lambda_+}\Big)^{|i-j|} \tag{1.53}$$

When multiplying $|i - j|$ by the lattice constant a, we can also see this as a function of distance r to find that correlations decay exponentially,

$$G(r) \sim e^{-r/\xi} , \tag{1.54}$$

on a characteristic length scale

$$\xi = (\ln \lambda_+ / \lambda_-)^{-1} . \tag{1.55}$$

This result is central as it extends to many other systems, as we will see. It might still happen that further, smaller length scales appear, but with increasing system size they will all be determined by the few highest eigenvalues of the tranfer matrix. In natural units, ξ has dimensions of a mass, which is why $1/\xi = m$ is sometimes referred to as the *mass gap* in a theory.

Summarising, in this section it has been shown that, while for $d = 1$ the Ising model exhibts only a zero temperature phase transition, for $d = 2$ and zero external field it additionally accomodates for one at a critical temperature T_c which depends on the interaction strength J and the lattice co-ordination number z. In the thermodynamic limit, the order parameter M_Ω changes continuously from zero to non-zero value at T_c. However, the *sign* of M_Ω in the ordered phase inherently supersedes our observation. A situation like this is known as *spontaneous symmetry breaking* and will be the topic of the following section.

1.1.4 Spontaneous symmetry breaking

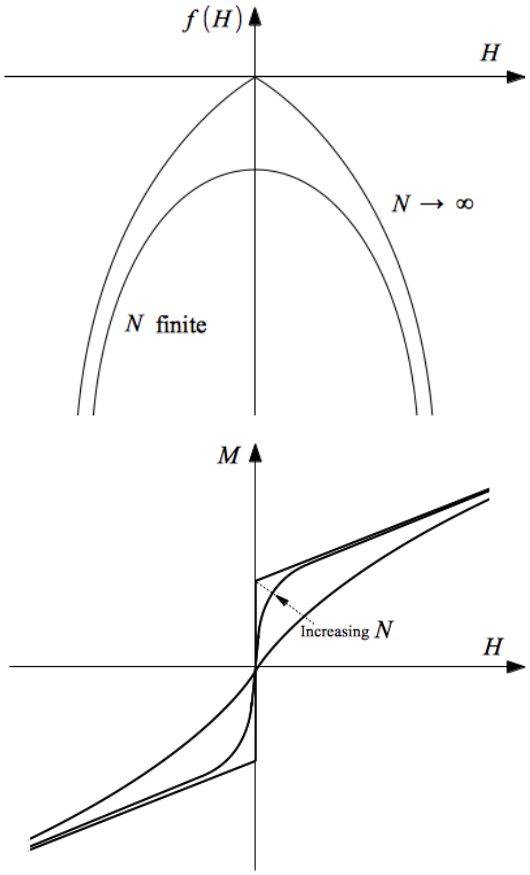

Figure 1.4: Free energy density (*top*) and magnetisation (*bottom*) as functions of the external magnetic field. The spontaneous magnetisation is temperature dependent as depicted in fig. 1.1.3.

Describing physical systems in terms of the symmetries they exhibit often leads to a great simplification in their theoretical description and at the same time provides a way to capture their characteristical behaviour. Often however, the symmetries are only approximately present in reality. In that case, one can still hope that a model incorporating the exact symmetry preserves a great part of predictional capacity. Going further, it could be that the states in which one observes the system do not even approximately reflect any symmetry. Even in that case, the conjecture could be that there are states, unobserved because at too high energies, that *are* invariant under certain symmetry transformations. This scenario is what the idea of spontaneous symmetry breaking puts into a general framework.

The first distinction one has to make is between discrete and continuous symmetries, which then each can be realised either globally or locally. The discrete case extends the discussion of the preceding section and is relevant in particular to con-

densed matter physics. The continuous case is very rich in theoretical consequences of general applicability. If locally present, it has direct effects on the particle spectrum of a theory. We begin with the first example, focussing again on the representative case of the Ising model from above.

Regarding the free energy density f as a function of the external field H only, the global $\mathbb{Z}_2$ symmetry we found in (1.26) meant that $f(H) = f(-H)$. From eqns. (1.14) and (1.19) it can further be concluded that $f(H)$ has to be concave, that is $f(\alpha H_1 + \beta H_2) \geq \alpha f(H_1) + \beta f(H_2)$ (c.f. 1.1.4). Particular interest lies on its analytical properties, especially at the origin. From the stated two properties it follows that

$$\frac{\partial f}{\partial H} \lesseqgtr 0 \text{ for } H \gtreqless 0\,. \tag{1.56}$$

Now, if f *were* differentiable then we could write

$$\lim_{\varepsilon\to 0} \frac{\partial f}{\partial H}\bigg|_{H=-\varepsilon} = \frac{\partial f}{\partial H}\bigg|_{H=0} = \lim_{\varepsilon\to 0} \frac{\partial f}{\partial H}\bigg|_{H=+\varepsilon} \tag{1.57}$$

and because of eqn. (1.56) one would be lead to find that the magnetisation is always zero in zero external field:

$$M(0) \equiv \frac{\partial f}{\partial H}\bigg|_{H=0} = 0 \quad \text{if} \quad f \in C^1 \tag{1.58}$$

But this cannot be true in general as we just showed in section 1.1.3 that in $d > 1$ there must exist a temperature T_c below which $M \neq 0$. The conclusion is that f is not differentiable, its first derivative exhibits a discontinuity at $H = 0$.

The $\mathbb{Z}_2$ symmetry must be broken by the transition at $H = 0$ because otherwise we would see no magnetisation. As there is no other than the technical argument above, this breaking of symmetry is said to happen spontaneously. What is more, the sign of the magnetisation below T_c is infinitely sensitive to the environment, making the outcome effectively unpredictable. This further justifies the terminology. The phenomenon of spontaneous symmetry breaking is clearly to be distinguished from the process of explicitly breaking a symmetry by tuning coupling constants, which in the case of the Ising model would simply mean changing from $H = 0$ to $H \neq 0$ for any $T > T_c$.

The general situation arising from the spontaneous breaking of a global, continuous symmetry was analysed first by Goldstone. His ideas will be presented here for the simplest case, a system invariant under the action of the one-parameter unitary group $U(1)$, which will be of direct relevance later in this work.

Let the Lagrangian density for a classical, complex scalar Ψ be

$$\mathcal{L}(\Psi, \Psi^*) = \partial^m \Psi^* \partial_m \Psi - U(\Psi^* \Psi) \tag{1.59}$$

where μ runs over time and space indices, $\mu = 0, ..., 3$, and Einstein convention is assumed – as it is subsequently. The potential is assumed to be of the form

$$U(\Psi^* \Psi) = -m^2 \Psi^* \Psi + \frac{\lambda}{2} (\Psi^* \Psi)^2\,, \tag{1.60}$$

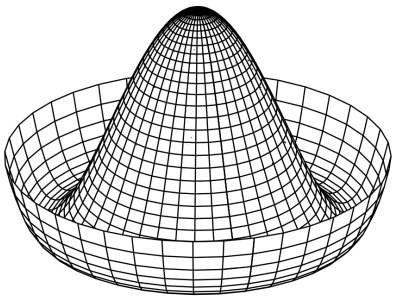

Figure 1.5: A typical potential giving rise to spontaneous symmetry breaking. It is sometimes referred to as 'mexican hat' or 'wine bottle' potential and has the standard form $V(\phi_1, \phi_2) = -a|\phi|^2 + b|\phi|^4$ for $a, b > 0$ and a two-component variable $\phi = (\phi_1, \phi_2)$ which often is a complex scalar field.

and hence only depends on the modulus of the field. Relativistic notation is applied here, although the following arguments do not rely on Lorentz invariance. $\mathcal{L}$ is symmetric under a global change of phase by a constant θ

$$\begin{aligned} \Psi &\longrightarrow \Psi \mathrm{e}^{ig\theta} \\ \Psi^* &\longrightarrow \Psi^* \mathrm{e}^{-ig\theta} \\ \Rightarrow \mathcal{L}(\Psi, \Psi^*) &\longrightarrow \mathcal{L}(\Psi \mathrm{e}^{ig\theta}, \Psi^* \mathrm{e}^{-ig\theta}) = \mathcal{L}(\Psi, \Psi^*) \end{aligned} \tag{1.61}$$

where g is some coupling constant. The Hamiltonian density is

$$\mathcal{H} = \partial^t \Psi^* \partial_t \Psi - \partial^i \Psi^* \partial_i \Psi + U(\Psi^* \Psi)\,. \tag{1.62}$$

In the non-relativistic setting, instead of $\mathcal{H}$ we would need to consider a thermodynamic potential at this point. This does however not alter the structure of the following argument so that for simplicity we may stick to only regarding the Hamiltonian. For systems exhibiting a continuous symmetry, Noether's theorem states that as long as the equations of motion hold,

$$\begin{aligned} \partial_\mu \frac{\partial \mathcal{L}}{\partial(\partial_\mu \Psi)} - \frac{\partial \mathcal{L}}{\partial \Psi} &= 0 \\ \partial_\mu \frac{\partial \mathcal{L}}{\partial(\partial_\mu \Psi^*)} - \frac{\partial \mathcal{L}}{\partial \Psi^*} &= 0\,, \end{aligned} \tag{1.63}$$

then for each independent symmetry transformation, that is, for every generator of the symmetry group, there exists a conserved current,

$$\partial^\mu J_\mu = 0\,. \tag{1.64}$$

One then identifies the respective charge Q carried by each J^m as

$$Q = \int \mathrm{d}^3 x\, J^0 \tag{1.65}$$

and, in the case of a Lie group symmetry, recognises them to be in turn the respective generator. In the $U(1)$ example defined in eqn. (1.61) the single Noether current is

$$J^\mu = -i\Big(\Psi^*\partial^\mu\Psi - \Psi\partial^\mu\Psi^*\Big)\,, \tag{1.66}$$

carrying charge $Q = 1$.

For $m^2 > 0$, the lowest energy states of the Hamiltonian (1.62) are infinitely degenerate and lie on the ring of potential minima in field space with radius

$$\rho_0 := \sqrt{\Psi^*\Psi}\Big|_{U\stackrel{!}{=}\min} = \frac{m}{\sqrt{\lambda}}\,. \tag{1.67}$$

The situation is similar to the $\mathbb{Z}_2$ case, only that the range of values the field can equivalently assume for the ground state is no longer twofold or even finite but has become on its own a smooth subspace $\mathcal{M}_0$ of the whole space of field configurations $\mathcal{M}$. Especially in particle physics, $\mathcal{M}_0$ is often referred to as the *vacuum manifold*, while in general the groundstates are not necessarily empty space. Here, $\mathcal{M}_0$ is a circle of $\rho_0 = const.$ and can be parametrised by the phase angle:

$$\mathcal{M}_0 = \Big\{p \in M \Big| (\Psi^*\Psi)|_p = \rho_0,\ \arg(\Psi) \in [0, 2\pi)\Big\} \tag{1.68}$$

Again, arbitrarily small, quantum or thermal fluctuation will inevitably make the system pick one point on the ring. Once it has chosen some ground state $(\rho_0,\, \theta_0)$, the $U(1)$ symmetry is lost. Although the current (1.66) is still conserved, its charge Q does no longer generate the symmetry but transports the field an infinitesimal amount $\delta\theta$ along the circle:

$$Q: \quad (\rho_0,\, \theta_0) \longmapsto (\rho_0,\, \theta_0 + \delta\theta)\,. \tag{1.69}$$

The masses M_{ij} in the theory are obtained from the second derivatives of the potential at the ground state,

$$M_{ij} = \frac{\partial^2 U}{\partial q_i \partial q_j}\bigg|_{(\rho_0,\,\theta_0)} \tag{1.70}$$

where the identification $q_1 := |\Psi|$ and $q_2 := \theta$ has been made. The crucial observation now is that $M_{22} = 0$. This means that a massless mode has entered the system, or, non-relativistically speaking, a mode excitable without having to overcome an energy gap. Massless modes arising from spontaneous symmetry breaking are called *Goldstone modes*. It is to be emphasised that spontaneous symmetry breaking only occurs due to the negative mass term in the potential. For a potential with all positive coefficients the global minimum lies at $\Psi = \Psi^* = 0$, which then is a stable point with all masses positive because it is invariant under the $U(1)$ action.

Goldstone's Theorem is the generalisation to the situation of a theory globally invariant under *any* continuous group G that is spontaneously broken to some subgroup $H \subset G$ leaving only the ground states invariant. Then the vacuum manifold $\mathcal{M}_0$ can be written as the coset

$$\mathcal{M}_0 = G/H\,. \tag{1.71}$$

In the simple case above we had $G = U(1)$ and H being the trivial group, so that the manifold of degenerate ground states became a circle: $\mathcal{M}_0 = U(1) \sim SO(2)$. The essence of Goldstone's theorem is that a massless mode will appear for *each* generator t_i of G that fails to leave the ground state invariant, meaning

$$\sum_k (t_i)_{jk} \Psi_k|_{p \in \mathcal{M}_0} \neq 0 \tag{1.72}$$

in some representation Ψ_k of G. Hence, the predicted number of massless particles equals $\dim\mathcal{M}_0 = \dim G - \dim H$. In case a symmetry was only approximately present initially, then the particles will be light at least. However, the theorem does not state a one-to-one correspondence between these so-called broken generators and massless (or light) particles but leaves open the possibility of accidentally vanishing zero modes of the mass matrix. In momentum space, the Goldstone modes – which are in fact bosonic — correspond to long wavelength excitations. As such, they are directly associated with the emergence of long-range interaction as observed in the Ising model in the preceding section. This potentially raises worries about finiteness in the infrared region of the energy spectrum and thus usually makes a theory subject to renormalisation, as will be seen later. Note lastly that we have left open the possibility of G describing not only internal but also Galilean or Lorentz symmetry. This is in fact the case for any crystal, in which case the lattice oscillations, described in terms of phonons, take the role of the Goldstone modes.

Finally, the case of a broken local, or gauge, symmetry has to be considered. The principle work on this has been done in the late 60s and early 70s by Kibble and others, eventually leading to the prediction of the Higgs boson. The central idea will be illustrated here again in terms of a simple abelian $U(1)$ model from above. But now, the symmetry transformations admit a space-dependent parameter $\theta \to \theta(\mathbf{x})$:

$$\begin{aligned} \Psi &\longrightarrow \Psi \mathrm{e}^{ig\vartheta(\mathbf{x})} \\ \Psi^* &\longrightarrow \Psi^* \mathrm{e}^{-ig\vartheta(\mathbf{x})} \end{aligned} \tag{1.73}$$

The type of Lagrangian density incorporating this symmetry relies on the introduction of a gauge field A_μ transforming as

$$A_\mu \longrightarrow A_\mu + \partial_\mu \vartheta \tag{1.74}$$

and has the shape

$$\mathcal{L}_{\mathrm{loc}} = D^\mu \Psi^* D_\mu \Psi - U(\Psi^* \Psi) \tag{1.75}$$

with *covariant derivatives*

$$\begin{aligned} D_\mu \Psi &= (\partial_\mu - ig\, A_\mu)\Psi \\ D_\mu \Psi^* &= (\partial_\mu + ig\, A_\mu)\Psi^* \,. \end{aligned} \tag{1.76}$$

We have omitted the gauge field's self-interaction

$$\mathcal{L}_{\mathrm{em}} = \frac{1}{4}(\partial^\mu A^\nu - \partial^\nu A^\mu)(\partial_\mu A_\nu - \partial_\nu A_\mu) \tag{1.77}$$

because it does not affect the discussion. $\mathcal{L}_{\rm em}$ is invariant against gauge transformations (1.74) and could simply be added to $\mathcal{L}_{\rm loc}$ for completeness. So far there is no mass term for the gauge field, but the symmetry breaking has not yet been considered. The potential $U(\Psi^*\Psi)$ is the same as in the preceding case and so we know already that the states of minimum energy will lie on a circle with non-zero radius in field space and that the system will pick one of them as the ground state. As before, we change coordinates from (Ψ, Ψ^*) to $(\rho, \theta) = (\sqrt{\Psi^*\Psi}, \arg\Psi)$ and choose to call the randomly chosen ground state to be lying at (ρ_0, θ_0). Taking $\theta_0 = 0$ without loss of generality and re-parametrising as

$$\Psi(x) = (\rho_0 + \rho(x))\mathrm{e}^{i\theta(x)/\rho_0} \tag{1.78}$$

we can write when close to (ρ_0, θ_0):

$$\Psi(x) = (\rho_0 + \rho(x) + i\theta(x)) + \mathcal{O}(\rho^2, \theta^2, \rho\theta) \tag{1.79}$$

The global $U(1)$ symmetry had been broken at this point, with $\theta(x)$ corresponding to the massless Goldstone mode. But now there remains a freedom to transform locally with $\vartheta(\mathbf{x}) = -\theta/\rho_0$ and thus *gauge the Goldstone away* at every point in spacetime:

$$\Psi(x) \longrightarrow \Psi'(x) = \mathrm{e}^{-\theta/\rho_0}\Psi(x) = \rho_0 + \rho(x) + \mathcal{O}(\rho^2) \tag{1.80}$$

However simultaneously the gauge field and with it the covariant derivative becomes

$$\begin{aligned} A_\mu &\longrightarrow A'_\mu = A_\mu - \frac{1}{\rho_0}\partial_\mu\theta \\ D_\mu &\longrightarrow D'_\mu = \partial_\mu - igA'_\mu \end{aligned} \tag{1.81}$$

so that the Lagrangian at the chosen point on $\mathcal{M}_0$ changes to

$$\begin{aligned} \mathcal{L}'_{\rm loc}|_{(\rho_0,0)} &= [D'^\mu(\rho_0 + \rho)]^*[D'_\mu(\rho_0 + \rho)] - U((\rho_0 + \rho(x))^2) \\ &= [D'^\mu\rho]^*[D'_\mu\rho] + g^2A'^\mu A'_\mu\rho_0(\rho_0 + 2\rho) - U(\rho^2) \\ &\quad - 2m^2\rho\rho_0 + \lambda(3\rho^2\rho_0^2 + 2\rho^3\rho_0) + \text{const.}. \end{aligned} \tag{1.82}$$

Strikingly, A_μ has acquired a mass of $\sqrt{2}g\rho_0$, while the Goldstone mode has disappeared completely, by virtue of a transverse polarisation of the gauge field. This is what is commonly referred to as the *Higgs mechanism*. This particular example is the theoretical basis for superconduction, where at the phase transition the electromagnetic field acquires its mass from merging with the phonons to form new quasi-particles – the Cooper pairs. The generalisation to the non-Abelian case lies at the heart of the Standard Model where $G = SU(3) \times SU(2) \times U(1)$ and, in the evolution of the universe, this product group is being broken in a sequence of phase transitions that leave the photon as the only exact vacuum Goldstone field known today.

1.2 Criticality

1.2.1 Mean fields and Landau theory

Phase transitions are the result of complex interactions between a large number of particles. It is an overwhelming and often impossible mathematical task to capture

the complete microscopic dynamics. Instead, one focusses on the description in terms of a suitable order parameter. Landau was the first to promote the idea that there might be a fairly general framework appropriate for a description like this and incorporated the ideas of mean-field theory to develop such a scheme for the description of critical phenomena. One can of course not expect that as such it will be correct for all values of parameters. In fact, its validity is severely constrained to the vicinity of second order phase transitions, that is to small values of $T - T_c$. An overview over Landau's approach will be given in the following.

First we realise that, if there exists a description suitable for a range of different systems, then this will need to be in terms of a field which varies on scales that are indifferent to the microscopic details. Thus we anticipate that a continuum description will be possible i.e. that the partition function can be converted to a functional integral over appropriately weighted field configurations. For now, we can leave open how this field will relate to a possible order parameter belonging to a specific transition. But what Landau demanded is that the field shall exhibit the same symmetries as the underlying system. For the Ising model this would mean invariance of the action against $\mathbb{Z}_2$ transformations and in fact we could introduce Landau's ideas simply by looking at a field $\Phi(\mathbf{r})$ with an action $S[-\Phi] = S[\Phi]$. However, it is not much more difficult to consider Φ to be complex and additionally demanding $U(1)$ invariance $S[\Phi^*] = S[\Phi]$. This has the virtue of directly connecting to our example of spontaneous symmetry breaking and will also provide insights into the Ginzburg-Landau theory of superconductivity, one of the major applications of the principles of Landau theory. The generalisation to other symmetries and more component fields is possible.

We start off by writing the partition function of a general system in equilibrium as

$$Z = \int \mathcal{D}\Phi^*(\mathbf{r})\mathcal{D}\Phi(\mathbf{r})\mathrm{e}^{-S[\Phi]} \tag{1.83}$$

with the action being of the simplest possible form incorporating the wanted symmetries:

$$S[\Phi] = \beta \int \mathrm{d}^d r \left[\frac{1}{2m} |\nabla\Phi(\mathbf{r})|^2 - \mu|\Phi(\mathbf{r})|^2 + \frac{\lambda}{2}|\Phi(\mathbf{r})|^4 \right] \tag{1.84}$$

The integration measure on the field space in eqn. (1.83) is only defined up to constant factors, which will cancel in any calculation of observables. Therefore it is enough to define it by the following short-hand notation:

$$\int \mathcal{D}\Phi(\mathbf{r}) \propto \int \prod_{a=1}^{d} \lim_{N_a\to\infty} \prod_{i_a=1}^{N_a} \mathrm{d}^d\Phi(\mathbf{r}_{i_1\ldots i_d}) \tag{1.85}$$

with space divided into a hyper-cubic grid consisting of $N_a \to \infty$ sites in the a-th dimension, labelled by $\{\mathbf{r}_{i_1\ldots i_d}\}$, and with infinitesimal distances between them being in the a-th dimension

$$(\mathrm{d}x^a)_i = \lim_{N_a\to\infty} \frac{|\mathbf{r}_{i_1..i_a+1\ldots i_d} - \mathbf{r}_{i_1..i_k\ldots i_d}|}{N_a}, \quad i = 1\ldots N_a \ . \tag{1.86}$$

The theory like this can be viewed as the time independent version of the standard path integral formulation of scalar field theory, with the time coordinate taken to be

imaginary. Bearing this in mind, we could just as well have called S the free energy of the system. The integral Z will pick up the most contributions from points where S is minimised. Hence a first step is to look at the theory for such configurations Φ_0 of the field that satisfy

$$\left.\frac{\delta S}{\delta \Phi}\right|_{\Phi_0} = 0\,. \tag{1.87}$$

This defines the *saddle-point approximation*. A phase transition induced by spontaneously broken symmetry is incorporated by assuming μ to be a tuning parameter behaving as

$$\mu \sim -(T - T_c) + \mathcal{O}((T - T_c)^2)\,. \tag{1.88}$$

Just as described in sec. 1.1.4, for $T > T_c$ μ is negative and eqn. (1.87) yields $\Phi_0 = 0$ while for $T < T_c$ μ is positive and $\Phi_0 = 0$ becomes a local maximum and S is minimised by all field configurations satisfying $|\Phi_0|^2 = \mu/\lambda$. The minimum value of the action is proportional to β and, because it is constant in space, to the volume V of the system:

$$S[|\Phi_0|] = \sqrt{\frac{\mu}{\lambda}} = -\beta V \frac{\mu^2}{2\lambda} \tag{1.89}$$

We have seen in the Ising model how the magnetic field couples linearly to the internal variables. In Landau theory the linear coupling of an external parameter is realised by the introduction of a source field $j(\mathbf{r})$ that modifies the action to

$$S[\Phi] \longrightarrow S[\Phi;\, j] + \int \mathrm{d}^d r \Big[\Phi(\mathbf{r}) j(\mathbf{r}) + c.\,c.\Big] \tag{1.90}$$

where the complex conjugate $\Phi^*(\mathbf{r}) j^*(\mathbf{r})$ is needed to preserve $U(1)$ symmetry in the action. Much like a one-dimensional Gaussian distribution is characterised by its variance, a central quantitiy to describe fluctuations in Φ is the susceptibility

$$\begin{aligned}
\chi(\mathbf{r}, \mathbf{r}') :&= \Big\langle \Big(\Phi(\mathbf{r}) - \big\langle \Phi(\mathbf{r}) \big\rangle\Big)^* \Big(\Phi(\mathbf{r}') - \big\langle \Phi(\mathbf{r}') \big\rangle\Big) \Big\rangle \\
&= \big\langle \Phi^*(\mathbf{r}) \Phi(\mathbf{r}') \big\rangle - \big\langle \Phi^*(\mathbf{r}) \big\rangle \big\langle \Phi(\mathbf{r}') \big\rangle \\
&= \big\langle \Phi^*(\mathbf{r}) \Phi(\mathbf{r}') \big\rangle - \big| \big\langle \Phi(\mathbf{r}) \big\rangle \big|^2
\end{aligned} \tag{1.91}$$

where again, the expectaion value is calculated analogously to the discrete discription, as the average over all configurations,

$$\big\langle ... \big\rangle = \frac{1}{Z} \int \mathcal{D}\Phi^*(\mathbf{r}) \mathcal{D}\Phi(\mathbf{r}) \,...\, \mathrm{e}^{-S[\Phi;\, j]}\,. \tag{1.92}$$

It can equally well be understood as the linear response to the external field as it is obtained via the derivative of Z with respect to the source:

$$\chi(\mathbf{r}, \mathbf{r}') = \left.\frac{\delta^2 \ln Z}{\delta j^*(\mathbf{r}) \delta j(\mathbf{r})}\right|_{j=0}. \tag{1.93}$$

In field theory, this would be referred to as as the connected two-point correlation function $G(\mathbf{r})$. In the common case, where systems are translationally invariant, one can anticipate that the susceptibility is only a function of the difference between coordinates, $\chi(\mathbf{r},\mathbf{r}') \to \chi(\mathbf{r}-\mathbf{r}')$. Deriving an analytic expression for it is non-trivial in general. For weak coupling however ($\lambda \ll 1$), and small fluctuations around Φ_0, S becomes approximately quadratic in Φ, so that the integral can be easily performed and we obtain an expression for the susceptibility around the saddle point. To this end, we first bring the free partition function

$$Z_0[\Phi;\, j] = \int \mathcal{D}\Phi^*(\mathbf{r})\mathcal{D}\Phi(\mathbf{r})\, \mathrm{e}^{-S_0[\Phi;j]} \tag{1.94}$$

to Gaussian form:

$$\begin{aligned} S_0[\Phi;\, j] &= \int \mathrm{d}^d r \left[\beta\Big(\frac{1}{2m}\nabla\Phi^*(\mathbf{r})\nabla\Phi(\mathbf{r}) - \mu\Phi^*(\mathbf{r})\Phi(\mathbf{r})\Big) + \Phi(\mathbf{r})j(\mathbf{r}) + \Phi^*(\mathbf{r})j^*(\mathbf{r})\right] \\ &= \int \mathrm{d}^d r \left[-\beta\Phi^*(\mathbf{r})\Big(\frac{1}{2m}\Delta + \mu\Big)\Phi(\mathbf{r}) + \Phi(\mathbf{r})j(\mathbf{r}) + \Phi^*(\mathbf{r})j^*(\mathbf{r})\right], \end{aligned} \tag{1.95}$$

assuming Φ to fall off at spatial infinity at least as fast as $1/|\mathbf{r}|$. Further, denoting Fourier transforms with a hat, we can write

$$\begin{aligned} S_0[\Phi;\, j] &= \int \mathrm{d}^d r \frac{\mathrm{d}^d k}{(2\pi)^d}\frac{\mathrm{d}^d k'}{(2\pi)^d}\, \mathrm{e}^{i\mathbf{k}\cdot\mathbf{r}}\mathrm{e}^{i\mathbf{k}'\cdot\mathbf{r}}\times \\ &\qquad \times\left[-\beta\hat{\Phi}^*(\mathbf{k})\Big(\frac{-k^2}{2m} + \mu\Big)\hat{\Phi}(\mathbf{k}) + \hat{\Phi}(\mathbf{k})\hat{j}(\mathbf{k}) + \hat{\Phi}^*(\mathbf{k})\hat{j}^*(\mathbf{k})\right] \\ &= \int \frac{\mathrm{d}^d k}{(2\pi)^d}\left[\beta\hat{\Phi}^*(-\mathbf{k})\Big(\frac{k^2}{2m} - \mu\Big)\hat{\Phi}(\mathbf{k}) + \hat{\Phi}(-\mathbf{k})\hat{j}(\mathbf{k}) + \hat{\Phi}^*(-\mathbf{k})\hat{j}^*(\mathbf{k})\right] \\ &= \int \frac{\mathrm{d}^d k}{(2\pi)^d}\left[\beta\Big(\frac{k^2}{2m} - \mu\Big)\left(\hat{\Phi}(-\mathbf{k}) + \frac{\hat{j}(-\mathbf{k})/\beta}{\frac{k^2}{2m}-\mu}\right)^*\left(\hat{\Phi}(\mathbf{k}) + \frac{\hat{j}(\mathbf{k})/\beta}{\frac{k^2}{2m}-\mu}\right)\right. \\ &\qquad \left. - \frac{\hat{j}^*(-\mathbf{k})\hat{j}(\mathbf{k})/\beta}{\frac{k^2}{2m}-\mu}\right] \end{aligned} \tag{1.96}$$

A shift by terms independent on Φ like

$$\begin{aligned} \hat{\Phi}(\mathbf{k}) &\longrightarrow \hat{\Phi}(\mathbf{k}) + \frac{\hat{j}(\mathbf{k})}{\frac{k^2}{2m}-\mu} \\ \hat{\Phi}^*(-\mathbf{k}) &\longrightarrow \hat{\Phi}^*(-\mathbf{k}) + \frac{\hat{j}^*(-\mathbf{k})}{\frac{k^2}{2m}-\mu} \end{aligned} \tag{1.97}$$

will have no effect on Z_0 and so it follows that

$$\begin{aligned} Z_0[\Phi;\, j] = \exp\left[\frac{1}{\beta}\int \frac{\mathrm{d}^d k}{(2\pi)^d}\frac{\hat{j}^*(-\mathbf{k})\hat{j}(\mathbf{k})}{\frac{k^2}{2m}-\mu}\right]\times \\ \times\int \mathcal{D}\hat{\Phi}^*(\mathbf{k})\mathcal{D}\hat{\Phi}(\mathbf{k})\exp\Big[\beta\int\frac{\mathrm{d}^d k}{(2\pi)^d}\Big(\frac{k^2}{2m}-\mu\Big)\hat{\Phi}^*(-\mathbf{k})\hat{\Phi}(\mathbf{k})\Big] \end{aligned} \tag{1.98}$$

where the last term of eqn. (1.96) was pulled of the integral as it only depends on the source fields and $\mathcal{D}\Phi^*(\mathbf{k})$, $\mathcal{D}\Phi(\mathbf{k})$ can be defined analogously to their counterparts in coordinate space in eqn. (1.85) and (1.86). The remaining functional integral does not depend on the sources and factorises into one-dimensional Gaussian integrals which can be solved ($\int \mathrm{d}x\, \mathrm{e}^{-x} = \sqrt{\pi}$). But only the first term is of interest to see how the field reacts on the sourcing fields. So we write

$$\ln Z_0[\Phi;\, j] = \frac{1}{\beta} \int \frac{\mathrm{d}^d k}{(2\pi)^d} \frac{\hat{j}^*(-\mathbf{k})\hat{j}(\mathbf{k})}{\frac{k^2}{2m} - \mu} + \text{const.}\,. \tag{1.99}$$

After returning to coordinate space this means

$$\ln Z_0[\Phi;\, j] = \frac{1}{\beta} \int \mathrm{d}^d r \mathrm{d}^d r'\, j^*(\mathbf{r}) \chi_0(\mathbf{r} - \mathbf{r}') j(\mathbf{r}) + \text{const.} \tag{1.100}$$

where we have introduced

$$\chi_0(\mathbf{r} - \mathbf{r}') = \int \frac{\mathrm{d}^d k}{(2\pi)^d} \frac{\mathrm{e}^{i\mathbf{k}\cdot(\mathbf{r}-\mathbf{r}')}}{\frac{k^2}{2m} - \mu} \tag{1.101}$$

as the *mean-field susceptibility*, valid for small fluctuations around the ground state, in the non-broken phase of a non-interacting system. Defining the *correlation length*

$$\xi := \frac{\hbar}{2m|\mu|} \tag{1.102}$$

we find the more comprehensive form

$$\chi_0(\mathbf{r}) = \frac{2m}{\beta\hbar^2} \frac{F(r/\xi)}{r^{d-2}} \tag{1.103}$$

where F is a dimensionless function only of distance, varying on the scale given by ξ:

$$F(x) = x^{d-2} \int \frac{\mathrm{d}^d k}{(2\pi)^d} \frac{\mathrm{e}^{i\mathbf{k}\cdot\mathbf{x}}}{1 + k^2} \tag{1.104}$$

From the last two equations we already see that correlations become isotropic near T_c. Within the range of our approximation, we set $|\mu| \sim (T - T_c)$ and realise that the scale ξ on which the susceptibility changes is divergent as

$$\xi \sim |T - T_c|^{-1}\,. \tag{1.105}$$

Correspondingly, the Fourier transform of ξ_0 itself becomes singular at $\mathbf{k} = 0$:

$$\hat{\chi}_0(\mathbf{k} = 0) = (\beta|\mu|)^{-1} \sim (T - T_c)^{-1} \tag{1.106}$$

We conclude that, without assuming much about the microscopic details of the system, we have discovered that the critical point gives rise to long range order. This was a central observation from our detailed discussion of the Ising model. If one is not willing to take this as a mere coincidence, then one is lead to the assumption of *universality*.

1.2.2 Critical exponents & Universality

It was an extraordinary experimental observation that widely different physical systems can show very similar behaviour in the vicinity of a phase transition, at their respective critical temperatures T_c. The conjecture that there might exist an underlying mechanism for this arose under the name of universality. To make this notion quantitatively meaningful one introduces *critical exponents*, which characterise the behaviour of macroscopic quantities near the transition. Two of them have just been calculated already in Landau theory, where the divergence of the correlation length and mean-field susceptibility were revealed. In general, ν is the exponent associated with the divergence of the correlation length with respect to the reduced temperature $\vartheta = (T - T_c)/T_c$ as it passes from positive to negative values through zero:

$$\xi \propto |\vartheta|^{-\nu} \,. \tag{1.107}$$

It is not immediately obvious why ξ should be symmetric at the critical point and for some models additional exponents for $\vartheta < 0$ are defined. But often there is experimental evidence enough to assume symmetry. While we found $\nu = 1$ for Landau theory, the correlation function near the critical point was derived to $\chi_0(r) = G(r) \sim F(r/\xi)/r^{d-2}$. Any departure from this form by a general, possibly time-dependent correlation function $G(r,t)$ is characterised in terms of the *anomalous dimension* η: via

$$G(r,t) = \frac{F_\pm(r/\xi(t))}{r^{d-2+\eta}} \tag{1.108}$$

where one allows a possible discontinuity at T_c to distinguish between F_+ and F_-. Equations like (1.107) and (1.108) are called *scaling laws* because they preserve their form at all different scales. Equivalently speaking, under a change of scale in the argument, the functional relationship stays the same up to a factor.

Scaling laws also apply to other quantities like the susceptibility of a system, or its specific heat. Accordingly, many further critical exponents are defined. But all these relations follow from the assumption that the free energy density itself obeys a scaling law near the critical point:

$$f(T,H) = |\vartheta|^{1/w} \Phi_\pm(H/|t|^{u/w}) \,. \tag{1.109}$$

This is of course a severe restriction, which is why criticality only appears in distinct regions of phase diagrams. For example, in magnetic systems the behaviour of the magnetisation m (for generality here assumed either to be defined per d.o.f. or volume) can then be written as

$$m = -\frac{\partial f}{\partial H}\Big|_{H=0} = (-\vartheta)^{\frac{1-u}{w}} \Phi'_-(0) \tag{1.110}$$

for $\vartheta < 0$ and $m \equiv 0$ for $\vartheta > 0$, which defines a further exponent

$$\beta = \frac{1-u}{w} \,. \tag{1.111}$$

We see from here that critical exponents are not all independent from each other and it becomes a matter of convenience which to use as the basic ones. It is possible to

derive more relations than eqn. (1.111) between the different exponents so that there remain only three independent critical exponents. Under a further assumption known as *hyperscaling* (c.f. table 1.1) this reduces to only two. For instance, we could take them to be ν and η and deduce all the others from these. The crucial point is that the values of critical exponents come in sets, each holding for a variety of different systems. The small number of different sets is referred to as *universality classes* and one of them is represented by the Ising model. In fact there are other universal quantities besides the critical exponents, as for instance the amplitude ratios between the observables' value on both sides of the transition, as they appear in the repsective scaling laws. Systems in the same universality class exhibit the same macroscopic behaviour at their transitions. Only very basic properties like the dimensionality of a model and its symmetry can affect to which class it belongs. Apart from the Ising universality class, two important other classes are represented by the XY and the Heisenberg model, which can be understood as extensions of the Ising model. While in the XY model, the spins are allowed to point in any direction in the plane instead of only up or down, the Heisenberg model comes closest to reality by allowing the spin directions vary continuously in three space dimensions. A table of critical exponents, their meaning as well as their experimentally obtained values is given in table 1.1.

Let us go back a step and reconsider what it actually *means* for a system to obey a series of scaling laws. The property of these laws to preserve their form at all scales implies that the systems they describe must appear to an observer identical irrespective of where on the scale he looks. Most of the scaling laws in the description of critical phenomena are formulated with respect to the dimensionless parameter $\vartheta = (T - T_c)/T_c$. This reflects the fact that the temperature itself comes with a natural scale associated with it in this context – the critical temperature T_c. We have seen the second characteristic quantity to be the correlation length ξ. This characteristic distance also directly scales with ϑ and so we could reformulate every scaling law in terms of it without doing any harm other than possibly rendering some of them dimensionful. A change in the argument by a constant factor can then be understood as the observer zooming into the system by the same amount. If the scaling laws hold true, then he will see exactly the same picture. The system is *self-similar*. This means, in conclusion, that $\xi(T)$ cannot possibly be the only relevant length scale in the system. If at some initial scaling level, say, the major fluctuations in the order parameter are perceived to happen on distances of the order of ξ_0, and, looking at smaller scales, the same picture appears, then the most prominent fluctuations at the new stage must happen at smaller distances of the order of $\xi < \xi_0$. This of course means nothing else but that ξ' was present from the beginning. Hence we realise that systems obeying scaling laws in the vicinity of their respective critical point are affected by processes happening at many different scales and the important observables obtain contributions from the dynamics on all them. This is not at all a trivial physical insight and lies on the origin of a very general theoretical framework of addressing problems in physics. The necessary set of diverse tools are summarised under the name of *renormalisation* and need a separate discussion. In fact, renormalisation will provide an answer to the question of how universality arises. One of the very first, and at the same time, most convincing pieces of experimental evidence for universality is shown in fig. 1.2.2. This already displayed an obvious discrepancy between the values calculated by formerly known approximation schemes such as the mean-field

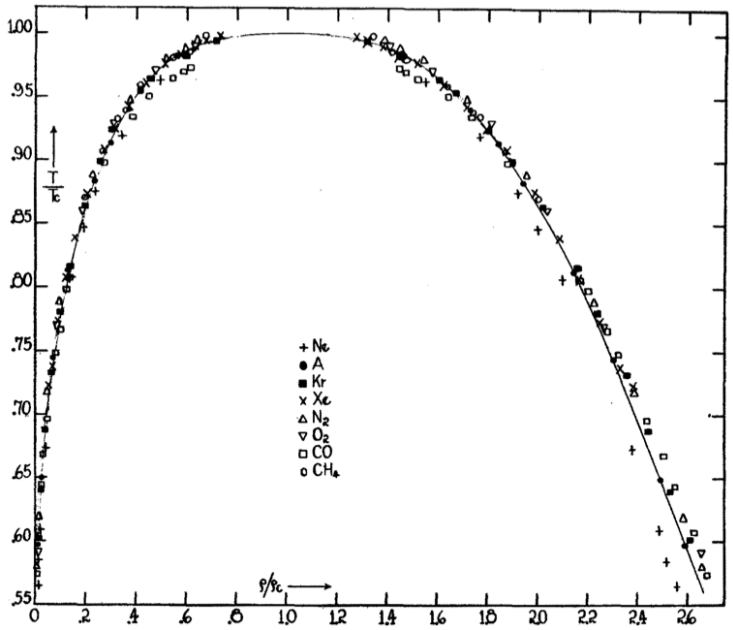

Figure 1.6: On the liquid-gas coexistence curve the mean-field theory predicts that, when rescaled with respect to their values at the critical point, the temperature should depend quadratically on the density. In contrast, the data displayed here suggests a cubic dependence, which is what renormalisation group calculations predict. By measuring this extremely similar behaviour of the different liquids near their critical point, Guggenheim provided overwhelming evidence for the existence of universality classes. (Reprinted with permission from [8].)

approach. Although inspired by the astonishing success of phenomenological theories like Landau's, renormalisation facilitates calculations which are able to predict, with high precision, values for critical exponents that agree with experiment.

1.2.3 Renormalisation group approach

One possible approach to the study of renormalisation is to ask how a generic theory changes when its smallest length scale increases. At first sight, this question might seem rather academic and of little practical use. But already within the limited account given here it will become clear how such a *coarse-graining* procedure leads to a better understanding of universality. A more detailed discussion can be found in [2] or [7].

Developed by Kadanoff in 1966 [9] for the two-dimensional Ising model, the block-spin method was one of the early approaches to the topic and it serves well in illustrating the basic ideas of renormalisation. The first step is to appreciate once again the situation at temperatures T near T_c: The distance $\xi(T)$ at which the spins correlate grows rapidly towards the critical point. This also means that, given the lattice spacing a, it should not be unreasonable to assume that there always is some integer

ℓ such that all spins separated by less than ℓa can be approximated to be acting as a single unit. The condition would only be that

$$a < \ell a \ll \xi(T)\,. \tag{1.112}$$

Then we can average over the obtained blocks I to obtain new spin variables S_I that assume the same values $S_I = \pm 1$ as the original ones. But of course, instead of N, one is now left with N/ℓ^2 block spins. One also must not forget to rescale all lengths that are measured in the lattice spacing. In particular, the correlation length of the block spins will have decreased like $\xi(T) \to \xi'(T) = \xi(T)/\ell$ and so the newly obtained system will be further apart from criticality. One step of blocking is depicted in fig. 1.2.3. Intuitively, we expect a single coarse-graining step of this kind not to affect the singular behaviour at the critical point because we know that that is due to the *long-range* interactions at scales of $\xi(T)$. What in this case we take as a further assumption, but in a more general picture appears as an approximation that can be systematically improved, is that the original Hamiltonian (1.19) may change under the described spin-blocking only in its coefficients, i.e.

$$H \equiv H_1(H_1, J_1) \longrightarrow H_\ell(H_\ell, J_\ell)\,, \tag{1.113}$$

but it will maintain its functional form. Inevitable for such a behaviour of the Hamiltonian under a change of fundamental scale will always be some rescaling prescription. This is why the prescription for transformations of this kind is usually referred to as a *renormalisation* scheme.

To make the notation more general, we write the set of coupling constants as $\mathbf{K}$. A general finite coarse-graining transformation on a system can then be expressed as

$$\mathbf{K}' = R_\ell[\mathbf{K}]\,, \tag{1.114}$$

where the transformation R_ℓ can and will often be non-linear. However, one requires that a change of scale by $\ell = \tilde{\ell}\ell$ should be equivalent to two successive changes by $\tilde{\ell}$ and ℓ,

$$\mathbf{K}'' = R_{\tilde{\ell}}[\mathbf{K}'] = R_{\tilde{\ell}} \cdot R_\ell[\mathbf{K}] \tag{1.115}$$

and thus

$$R_{\tilde{\ell}}[\mathbf{K}] = R_{\tilde{\ell}} \cdot R_\ell[\mathbf{K}]\,. \tag{1.116}$$

This last property explains the term *renormalisation group*, although strictly the transformations R_ℓ only form a semi-group as an inverse can in general not be defined. An important property of renormalisation group transformations is that they admit *fixed points* $\mathbf{K}^*$ for which

$$\mathbf{K}^* = R_\ell[\mathbf{K}^*]\,. \tag{1.117}$$

For these particular values of the coupling constants the correlation length must obey

$$\xi[\mathbf{K}^*] = \xi[\mathbf{K}^*]/\ell\,. \tag{1.118}$$

This can only possibly be true either for $\xi[\mathbf{K}^*] = 0$ or $\xi[\mathbf{K}^*] = \infty$. Fixed points with vanishing correlation length are called *trivial* and an obvious example is given by

$\mathbf{K} = \mathbf{0}$. The major insight however is that those fixed point with diverging correlation length each correspond to a critical point in some phase transition. Therefore they are called *critical fixed points*. In fact, it is straightforward to see that all points $[\mathbf{K}_c]$ for which $\lim_{N\to\infty} R_\ell^N[\mathbf{K}_c] = [\mathbf{K}^*]$ must already have exhibited an infinite correlation length, $\xi[\mathbf{K}_c] = \infty$. The set of all these point is called the *basin of attraction* of the critical fixed point $\mathbf{K}^*$ and its existence is responsible for universality. Although for discrete models like the Ising model it does not seem beneficial, it is a generalisation to allow ℓ to vary continuously. An infinitesimal renormalisation group transformation is obtained from eqn. (1.114) by setting $\ell \to (1+\epsilon)$ with $\epsilon \ll 1$. Labelling $\mathbf{K}_\ell \equiv R_\ell \mathbf{K}_1$ one can define

$$\frac{\mathrm{d}\mathbf{K}_l}{\mathrm{d}\ell} = \lim_{\epsilon\to 0} \frac{\mathbf{K}_{(1+\epsilon)\ell} - \mathbf{K}_\ell}{\epsilon\ell} \tag{1.119}$$

to find that the flow equation becomes

$$\frac{\mathrm{d}\mathbf{K}_\tau}{\mathrm{d}\tau} = B[\mathbf{K}_\tau] \tag{1.120}$$

where $\tau := \ln \ell$ and the transformation B has been defined by

$$B[\mathbf{K}_\ell] := \left.\frac{\partial R_{(1+\epsilon)}[\mathbf{K}_\ell]}{\partial \epsilon}\right|_{\epsilon=0} . \tag{1.121}$$

Fixed points satisfy

$$B[\mathbf{K}^*] = 0\,. \tag{1.122}$$

Because eqn. (1.120) is first order in τ, for given B, any initial point determines the trajectory completely and in particular its endpoint at $\tau \to \infty$. The basin of attraction of a critical fixed point can thus be understood as a *critical manifold*. Systems exhibiting critical behaviour correspond to points near but not on a critical manifold. Following the renormalisation group flow, their correlation length decreases and eventually one will be able to perform ordinary perturbation theory. Due to the one-to-one correspondence between final and initial points of any trajectory not lying on the critical manifold, one can then map the obtained results to the system one started with. This, in short, is the virtue of the renormalisation group.

Finally, let us see how in principle the local flow behaviour ultimately gives rise to scaling at the critical fixed points and how this connects to universality. Consider $\mathbf{K}$ to be in the neighbourhood of the critical fixed point $\mathbf{K}^*$, separated only by $\delta\mathbf{K}$, and another point $\mathbf{K}' = \mathbf{K}^* + \delta\mathbf{K}'$ generated via RG transformation R. Then we can expand

$$\begin{aligned} \mathbf{K}^* + \delta\mathbf{K}' = R[\mathbf{K}] &= R[\mathbf{K}^* + \delta\mathbf{K}] \\ &= R[\mathbf{K}^*] + \delta\mathbf{K} \cdot \left.\frac{\partial R[\tilde{\mathbf{K}}]}{\partial \tilde{\mathbf{K}}}\right|_{\tilde{\mathbf{K}}=\mathbf{K}^*} + \mathcal{O}(\delta\mathbf{K}^2) \end{aligned} \tag{1.123}$$

and hence, using $\nabla R[\mathbf{K}] \equiv \partial R[\tilde{\mathbf{K}}]/\partial\tilde{\mathbf{K}}|_{\tilde{\mathbf{K}}=\mathbf{K}}$ to denote the vector gradient in coupling constant space, we have

$$\delta\mathbf{K}' = \nabla R[\mathbf{K}^*] \cdot \delta\mathbf{K}\,. \tag{1.124}$$

Note that in the earlier notations, $B[\mathbf{K}] = (\frac{\partial \tilde{\mathbf{K}}}{\partial \epsilon} \cdot \nabla R_{1+\epsilon}[\tilde{\mathbf{K}}])|_{\tilde{\mathbf{K}}=\mathbf{K}}$. For simplicity, we assume $\nabla R(\mathbf{K}^*)$ to be symmetric and having eigenvalues β_n corresponding to eigenvectors $\mathbf{e}_n$,

$$\nabla R[\mathbf{e}_n] = \beta_n \mathbf{e}_n \,, \tag{1.125}$$

and rewrite $\delta\mathbf{K}$ and $\delta\mathbf{K}'$ in terms of this basis:

$$\begin{aligned} \delta\mathbf{K} &= \sum_n h_n \mathbf{e}_n \\ \delta\mathbf{K}' &= \sum_n h'_n \mathbf{e}_n \end{aligned} \tag{1.126}$$

Here, the coefficients h_n and h'_n correspond to the scaling fields, or variables, from the earlier phenomenological discussion of scaling. And indeed we can see this by noting from eqn. (1.124) that

$$h'_n = \beta_n h_n \tag{1.127}$$

and rewriting this as

$$h'_n = b^{\delta_n} h_n \tag{1.128}$$

with $\delta_n = \ln \beta_n / \ln b$. In those directions n in which $|h_n|$ increases under RG transformations near the critical fixed point, that is for $\delta_\alpha > 0$, h_n is called a *relevant* variable. If on the other hand $\delta_n < 0$, then n labels a direction in which $|h_n|$ decreases. In that case h_n is called an *irrelevant* variable and it will eventually tend to zero. *Marginal* variables correspond to $\delta_n = 0$ and lead to logarithmic corrections to scaling. The number of irrelevant variables is equal to the dimension of the critical manifold, while the number of relevant variables is called its *codimension*. It equals the number of parameters that have to be tuned in order for the system to undergo a phase transition. The central point is that each δ_n that corresponds to a relevant variable determines one critical exponent and because under RG group transformations all points on the critical surface merge to the same fixed point, the critical exponents will be the same for all of them. Each universality class is thus associated with one critical manifold.

Although one could in principle allow for further external fields, the Ising model as we introduced it had coupling constants that were functions of T and H. both of them had to be tuned to induce a continuous phase transition. Hence the critical manifold was zero-dimensional – a point in the phase diagram.

The discussion in this section focussed on the real space renormalisation group to provide an illustrative and immediate access to the main ideas. Equivalently and in the same spirit, one defines a realisation in momentum space. Coarse-graining there corresponds to integrating out those degrees of freedom with the highest momenta and the renormalisation group flow is being generated by continuously lowering the corresponding cutoff. While the basic ideas are the same, this approach enables the development of direct, perturbative calculation schemes for the partition function, that are of general applicability.

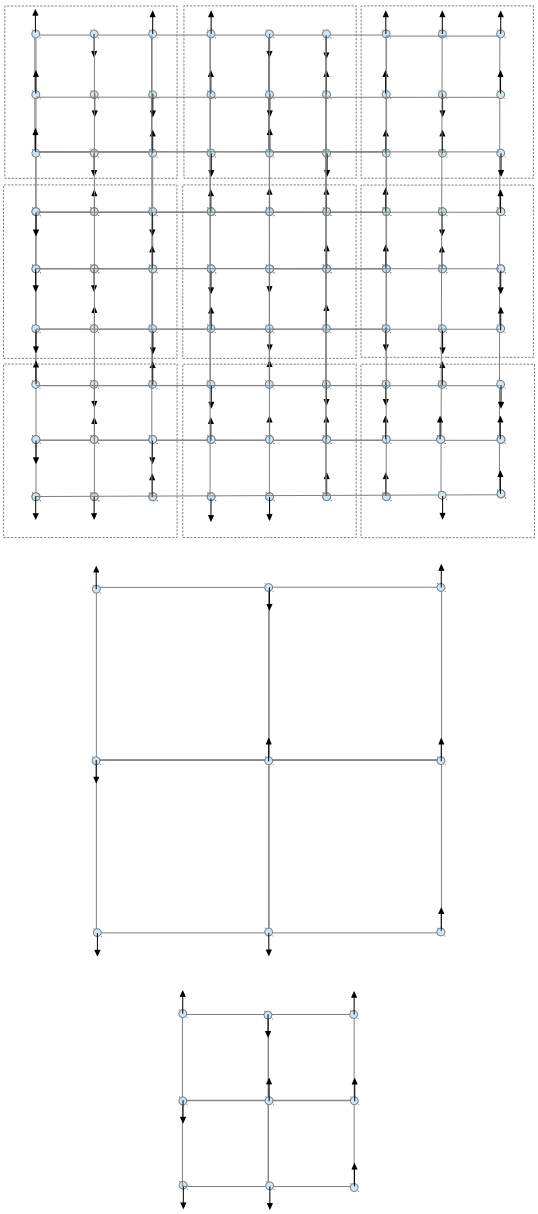

Figure 1.7: The block-spin method is a simple example for a renormalisation group operation. It means coarse-graining the $2d$-Ising lattice by a factor of 2, shown here for a representative 9×9-block. First, the magnetisation is averaged over 3×3 blocks of spins to obtain a new lattice with twice the original lattice constant. Afterwards one needs to 'zoom out' by a factor of 2 to make the coarse grained lattice appear as the original one.

Exponent	Associated quantity in paramagnetic-ferromagnetic phase transition (2nd order)	Associated quantity in liquid-gas phase transition (1st order)	Relations	Numerical Values in Universality classes Ising(Xe) / XY(^{4}He) / Heisenberg(Ni)
α	Specific heat at $V = \text{const.}$ $C_V = -T\frac{\partial^2 f}{\partial T^2}\big\vert_{H=0}$	Specific heat at $V = \text{const.}$ $C_V = -T\frac{\partial^2 f'}{\partial T^2}\big\vert_{H=0}$	$\alpha = 2 - \frac{1}{w}$	$(< \ 0.2)/(-0.0127 \pm 0.0003)/(0.04 \pm 0.12)$
β	Magnetisation $m = -\frac{\partial f}{\partial H}\big\vert_{H=0}$	Red. dens. difference on coexist. curve $\Delta\rho = (\rho_L - \rho_G)/\rho_c$ [**]	$\beta = \frac{1-u}{w}$	$(0.35 \pm 0.015)/(-)/(0.358 \pm 0.003)$
γ	Uniform magnetic susceptibility $\chi \equiv \hat{\chi}(\mathbf{k}=0) = -\frac{\partial^2 f}{\partial H^2}\big\vert_{H=0}$	Compressibility at $T = \text{const.}$ $K_T = \frac{1}{\rho}\frac{\partial \rho}{\partial p}$	$\gamma = \frac{2u-1}{w}$	$(1.3 \pm 0.2)/(-)/(1.33 \pm 0.02)$
δ [*]	$m \propto H^{1/\delta}$	Reduced pressure at $T = \text{const.}$ $\Delta p = (p - p_c)/p_c = \Delta\rho^\delta$	$\delta = \frac{u}{1-u}$	$(4.3 \pm 0.5)/(-)/(4.29 \pm 0.05)$
η [*]	$\chi \propto \xi^{2-\eta}$ and Correl. fnc. [***] $G(r,t) = \langle (m(\mathbf{r})m(0)\rangle - m^2 \propto r^{-(d-2+\eta)}$	$\chi \propto \xi^{2-\eta}$ and Correl. fnc. [***] $G(r,t) = \langle (\rho(\mathbf{r})\rho(0)\rangle - \rho^2 \propto \rho^{-(d-2+\eta)}$	–	$(0.1 \pm 0.1)/(-)/(0.041 \pm 0.01)$
ν	Correlation length ξ	Correlation length ξ'	$\nu = \frac{\gamma}{(2-\eta)}$	$(\approx \ 0.57)/(0.6705 \pm 0.0006)/(0.64 \pm 0.1)$
u	Free energy density $f(T,H)$, c. f. eqn. (1.109)	Free energy density $f'(T,p)$	–	–
w	Free energy density $f(T,H)$, , c. f. eqn. (1.109)	Free energy density $f'(T,p)$	–	–
Hyperscaling if $f^{(\prime)} \propto (\xi^{(\prime)})^{-d}$:		$\alpha = 2 - \nu d$ (Josephson's law)		

Table 1.1: Critical exponents, their meaning near two types of critical points and measured values for representatives of three different universality classes [7]. If not indicated otherwise [*], then scaling is assumed with respect to $\vartheta = (T - T_c)/T_c$, i. e. for quantity q and critical exponent c, $q \propto |\vartheta|^{\tilde{\vartheta}}$ so that for positive values of critical exponents one finds a divergence. Only β is introduced as $m, \Delta\rho \propto |\vartheta^{+\beta}|$, because the order parameter stays finite during a continuous phase transition. Either two or three critical exponents remain independent, depending on whether hyperscaling holds true. [**]: Here really *equality* holds: $\Delta\rho = (-t)^{-\beta}$ (β only defined for $t < 0$). [***]: $\rho(\mathbf{r})$ and $m(\mathbf{r})$ are the locally defined versions of ρ and m.

2. Non-equilibrium: Defect formation

2.1 Fluctuation-Dissipation-Theorem

In this section a first attempt is made to study in greater detail the general effect of fluctuations around the equilibrium of a classical field. By constraining ourselves to small deviations, we will see that the relaxation behaviour to first order is independent of whether the fluctuations are spontaneous or if they are caused by external forces. The equations we obtain will be central to our aim of obtaining a time-dependent Landau theory that will provide a suitable first handle to compare our results from equilibrium to the critical behaviour of realistic systems. The general ideas contained in the subsequent passages are developed in orientation along [10], with the phase space formulation of statistical mechanics employed there being translated into field theoretic language here in order to match our way of introducing Landau theory.

We start by investigating the notion of a dynamical susceptibility for a real scalar field Φ, for which we write the partition function as

$$Z_0 = \int \mathcal{D}\Phi \, \mathrm{e}^{-\beta H_0[\Phi]} \tag{2.1}$$

with a generic Hamitonian given by H_0. The expectation value of the field in equilibrium is

$$\langle \Phi(\mathbf{x}) \rangle_0 := \int \mathcal{D}\Phi \, \rho_0[\Phi] \, \Phi(\mathbf{x}) \tag{2.2}$$

with the equilibrium probability distribution being

$$\rho_0[\Phi] = \frac{\mathrm{e}^{-\beta H_0[\Phi]}}{Z_0} \, . \tag{2.3}$$

Fluctuations around this value can be introduced via perturbations to the Hamiltonian so that

$$H_0 \to H = H_0 + H' \tag{2.4}$$

where the simplest form for H' we can assume is

$$H' = - \int \mathrm{d}^d x \, J(\mathbf{x}) \Phi(\mathbf{x}), \tag{2.5}$$

the source term from the Landau discussion. In this context, $J(\mathbf{x})$ can be seen as an *external force*, or on a more technical level, a generalised Lagrange multiplier. In contrast to averages $\langle ... \rangle_0$ computed in equilbrium as represented by eqn. (2.3), expectation values under the perturbed Hamiltonian will be denoted as

$$\langle ... \rangle = \int \mathcal{D}\Phi \, ... \, \rho[\Phi] \tag{2.6}$$

with probability density

$$\rho[\Phi] = \frac{\mathrm{e}^{-\beta H[\Phi]}}{Z} \,, \tag{2.7}$$

where Z is the partition function from eqn. (2.2) with H_0 being replaced by H. Asking how small changes in J shift the field expectation value we calculate

$$\begin{aligned}
\frac{\delta}{\delta J(\mathbf{y})} \langle \Phi(\mathbf{x}) \rangle &= \frac{\delta}{\delta J(\mathbf{y})} \frac{\int \mathcal{D}\Phi \, \Phi(\mathbf{x}) \, \mathrm{e}^{-\beta H_0} \big(1 + \beta \int \mathrm{d}^d x' \, J(\mathbf{x}') \Phi(\mathbf{x}') + \mathcal{O}(J^2)\big)}{\int \mathcal{D}\Phi \, \mathrm{e}^{-\beta H_0} \big(1 + \beta \int \mathrm{d}^d x' \, J(\mathbf{x}') \Phi(\mathbf{x}') + \mathcal{O}(J^2)\big)} \\
&= \frac{\delta}{\delta J(\mathbf{y})} \frac{Z_0 \big\langle \Phi(\mathbf{x}) \big\rangle_0 + Z_0 \beta \big\langle \Phi(\mathbf{x}) \int \mathrm{d}^d x' \, J(\mathbf{x}') \Phi(\mathbf{x}') \big\rangle_0 + \mathcal{O}(J^2)}{Z_0 + Z_0 \beta \big\langle \int \mathrm{d}^d x' \, J(\mathbf{x}') \Phi(\mathbf{x}') \big\rangle_0 + \mathcal{O}(J^2)} \\
&= \frac{\delta}{\delta J(\mathbf{y})} \Big[\big\langle \Phi(\mathbf{x}) \big\rangle_0 + \beta \Big\langle \Phi(\mathbf{x}) \int \mathrm{d}^d x' \, J(\mathbf{x}') \Phi(\mathbf{x}') \Big\rangle_0 \\
&\qquad\qquad - \beta \big\langle \Phi(\mathbf{x}) \big\rangle_0 \Big\langle \int \mathrm{d}^d x' \, J(\mathbf{x}') \Phi(\mathbf{x}') \Big\rangle_0 + \mathcal{O}(J^2) \Big] \\
&= \beta \Big[\big\langle \Phi(\mathbf{x}) \Phi(\mathbf{y}) \big\rangle_0 - \big\langle \Phi(\mathbf{x}) \big\rangle_0 \big\langle \Phi(\mathbf{y}) \big\rangle_0 + \mathcal{O}(J) \Big] \\
&= \beta \Big\langle \big(\Phi(\mathbf{x}) - \langle \Phi(\mathbf{x}) \rangle_0 \big) \big(\Phi(\mathbf{y}) - \langle \Phi(\mathbf{y}) \rangle_0 \big) \Big\rangle_0 + \mathcal{O}(J) \\
&\equiv \beta \big\langle \delta\Phi(\mathbf{x}) \delta\Phi(\mathbf{y}) \big\rangle_0 + \mathcal{O}(J) \\
&\equiv \beta \big\langle \Phi(\mathbf{x}) \Phi(\mathbf{y}) \big\rangle_c + \mathcal{O}(J)
\end{aligned} \tag{2.8}$$

where we have given a name to fluctuations around the equilibrium, $\delta\Phi(\mathbf{x}) := \Phi(\mathbf{x}) - \langle \Phi(\mathbf{x}) \rangle_0$, and now recognise the (equilibrium connected) two-point correlation function, or susceptibility $G(\mathbf{x}, \mathbf{y}) = \chi(\mathbf{x}, \mathbf{y}) = \big\langle \Phi(\mathbf{x}) \Phi(\mathbf{y}) \big\rangle_c$ that we already encountered in equations (1.91) — (1.93). Taking the limit $J \to 0$ in eqn. (2.8), we can then expand $\langle \Phi(\mathbf{x}) \rangle$ in the following way up to linear order in J:

$$\begin{aligned}
\langle \Phi(\mathbf{x}) \rangle &= \langle \Phi(\mathbf{x}) \rangle_0 + \int \mathrm{d}^d y \, J(\mathbf{y}) \frac{\delta \langle \Phi(\mathbf{x}) \rangle}{\delta J(\mathbf{y})} \Big|_{J=0} + \mathcal{O}(J^2) \\
&= \langle \Phi(\mathbf{x}) \rangle_0 + \beta \int \mathrm{d}^d y \, J(\mathbf{y}) \big\langle \delta\Phi(\mathbf{x}) \delta\Phi(\mathbf{y}) \big\rangle_0 + \mathcal{O}(J^2) \\
&= \langle \Phi(\mathbf{x}) \rangle_0 - \beta \big\langle \Phi(\mathbf{x}) H' \big\rangle_c + \mathcal{O}(J^2)
\end{aligned} \tag{2.9}$$

From here the conclusion is, that in a linear approximation for the perturbations, they in turn only linearly affect the shift of averages away from the equilibrium values. This is an example for the behaviour of system being captured within a *linear response* theory.

Now, we go on and wish to explore the relaxation properties of the system once the perturbations have vanished. This means that now we have to consider an explicit time dependence in the field, $\Phi(\mathbf{x}) \to \Phi(\mathbf{x}, t)$. For simplicity, the perturbations are assumed to be turned off instantaneously at the time $t = 0$. That is, the new perturbative part of the Hamiltonian will be

$$H'(t) = H'\Theta(-t) = \begin{cases} H', & t < 0 \\ 0, & t \geq 0 \end{cases} . \tag{2.10}$$

As before, we will restrict the discussion to small perturbations, so that we can rely on a linear approximation. Then, for $t < 0$ the field expectation value reduces to its time-independent form which we already calculated in eqn. (2.9). For positive times however, $\Phi(\mathbf{x}, t)$ obeys Liouvillian time evolution determined by the unperturbed Hamiltonian $H(t \geq 0) = H_0$:

$$\frac{\partial \Phi}{\partial t}(\mathbf{x}, t) = \left\{ \Phi(\mathbf{x}, t), H_0 \right\}, \quad t > 0 \tag{2.11}$$

where the field-theoretical Poisson bracket is

$$\left\{ \Phi(\mathbf{x}, t), H_0 \right\} = \frac{\delta H_0}{\delta \Phi(\mathbf{x}, t)} - \nabla \cdot \frac{\delta H_0}{\delta \nabla \Phi(\mathbf{x}, t)} + \partial_t \frac{\delta H_0}{\delta \partial_t \Phi(\mathbf{x}, t)} \tag{2.12}$$

Given a Hamiltonian H_0, the field configuration at $t = 0$, denoted as Φ_I, will completely determine its configuration at a time t. So we can label the solutions to eqn. (2.11) by Φ_I and write

$$\Phi(\mathbf{x}, t;\, \Phi_I) = \Phi_I(\mathbf{x}) + \int_0^t \mathrm{d}t' \left\{ \Phi(\mathbf{x}, t'), H_0 \right\} \tag{2.13}$$

We then obtain $\langle \Phi(\mathbf{x}, t) \rangle$ by averaging, with the probability density $\rho[\Phi_I]$ at t=0, over all initial field configurations Φ_I which have been evolved in time according to eqn. (2.13):

$$\left\langle \Phi(\mathbf{x}, t) \right\rangle = \int \mathcal{D}\Phi_I \, \rho[\Phi_I] \Phi(\mathbf{x}, t;\, \Phi_I) \tag{2.14}$$

From eqn. (2.9) it follows that the difference to the equilibrium value at $t = 0$ (or any other $t < 0$) has an expectation value of

$$\begin{aligned} \langle \delta\Phi(\mathbf{x}, t) \rangle &\equiv \langle \Phi(\mathbf{x}, t) \rangle - \langle \Phi(\mathbf{x}) \rangle_0 \\ &= \beta \int \mathrm{d}^d y \, J(\mathbf{y}) \langle \Phi(\mathbf{x}, t) \Phi(\mathbf{y}, 0) \rangle_c = \beta \int \mathrm{d}^d y \, J(\mathbf{y}) \langle \delta\Phi(\mathbf{x}, t) \delta\Phi(\mathbf{y}, 0) \rangle_0 . \end{aligned} \tag{2.15}$$

Note that $\Phi(\mathbf{x}, 0) \equiv \Phi(\mathbf{x})$ so that at $t = 0$ we recover eqn. (2.9) exactly. Here one identifies the *relaxation* (or *Kubo*) *function* $C(\mathbf{x}, \mathbf{y}, t)$ to be

$$C(\mathbf{x}, \mathbf{y}, t) = \langle \Phi(\mathbf{x}, t) \Phi(\mathbf{y}, 0) \rangle_c = \langle \delta\Phi(\mathbf{x}, t) \delta\Phi(\mathbf{y}, 0) \rangle_0 \tag{2.16}$$

which is the analogue of $G(\mathbf{x}, \mathbf{y})$ but now measures not the correlation of fluctuations around equilibrium in space but in time. Eventually the system is expected to reach

equilibrium, so $C(\mathbf{x},\mathbf{y},t\to\infty)=0$, and again we expect not to lose anything by anticipating $C(\mathbf{x},\mathbf{y},\,t,t')\equiv C(\mathbf{x}-\mathbf{y},\,t-t')$.

The meaning of eqn. (2.15) is that the relaxation of a slightly perturbed system back towards equilibrium is in turn determined only by equilibrium fluctuations. Interestingly, it does not matter whether the perturbation is spontaneously produced or the result of external forces.

In order to measure fluctuations both in space and in time, the *dynamical susceptibility* $\chi(\mathbf{x},\mathbf{y},\,t,t')$ is defined from the most general ansatz for a linear response to an external perturbation, which is now allowed to have explicit time dependence ($J(\mathbf{x})\to J(\mathbf{x},t)$):

$$\begin{aligned}\langle\delta\Phi(\mathbf{x},t)\rangle &= \int \mathrm{d}^d y \int_{-\infty}^{t} \mathrm{d}t'\,\tilde{\chi}(\mathbf{x},\mathbf{y},\,t,t')J(\mathbf{y},t') \\ &= \int \mathrm{d}^d y \int_{-\infty}^{\infty} \mathrm{d}t'\,\chi(\mathbf{x},\mathbf{y},\,t,t')J(\mathbf{y},t') \end{aligned} \tag{2.17}$$

We have chosen here to write $\chi(\mathbf{x},\mathbf{y},\,t,t')=\tilde{\chi}(\mathbf{x},\mathbf{y},\,t,t')\Theta(t-t')$ in order to understand causality as contained in the susceptibility and not making it explicit in the equations. For the non-dynamical susceptibility we found that in translationally invariant systems it is only dependent on the difference of coordinates. We further assume energy conservation, i.e. that translational invariance extends to the time coordinate, and hence we can write $\chi(\mathbf{x},\mathbf{y},\,t,t')\equiv\chi(\mathbf{x}-\mathbf{y},\,t-t')$. For $J(\mathbf{x},t)=J(\mathbf{x})\Theta(-t)$ as discussed above we can write

$$\begin{aligned}\langle\delta\Phi(\mathbf{x},t)\rangle &= \int \mathrm{d}^d y\, J(\mathbf{y},t) \int_{-\infty}^{0} \mathrm{d}t'\,\chi(\mathbf{x}-\mathbf{y},\,t-t') \\ &= \int \mathrm{d}^d y\, J(\mathbf{y}) \int_{t}^{\infty} \mathrm{d}\tau\,\chi(\mathbf{x}-\mathbf{y},\,\tau) \end{aligned} \tag{2.18}$$

Taking the time derivative

$$\frac{\mathrm{d}}{\mathrm{d}t}\langle\delta\Phi(\mathbf{x},t)\rangle = -\int \mathrm{d}^d y\, J(\mathbf{y})\chi(\mathbf{x}-\mathbf{y},\,t) = \beta\int \mathrm{d}^d y\, J(\mathbf{y})\Theta(t)\frac{\partial}{\partial t}C(\mathbf{x},\mathbf{y},t) \tag{2.19}$$

and comparing to the definition of the Kubo function in eqns. (2.15) and (2.16), the conclusion is that the dynamical susceptibility is just proportional to the time derivative of the Kubo function

$$\chi(\mathbf{x}-\mathbf{y},\,t) = -\beta\Theta(t)\dot{C}(\mathbf{x}-\mathbf{y},t)\,. \tag{2.20}$$

Having established this result, we are not far from understanding how the relaxation process for equilibrium fluctuations can be understood in dissipative terms. The way leading there employs the analyticity properties of $\chi(\mathbf{x},\mathbf{y},\,t,t')$.

In order to simplify the subsequent purely mathematical discussion, we make a physical assumption. This is that the equilibrium fluctuations we wish to describe are *uncorrelated* in space, so that we can write

$$\chi(\mathbf{x},\mathbf{y},\,t,t') = \delta^d(\mathbf{x}-\mathbf{y})\chi(t) \tag{2.21}$$

and thus limit the following discussion to a single point $\mathbf{x}_0$, denoting $\Phi(\mathbf{x}_0,t)\equiv\phi(t)$ and $J(\mathbf{x}_0,t)\equiv j(t)$, but also $C(\mathbf{x}-\mathbf{y},\,t-t')\to C(t)$ by the same argument as for the

susceptibility, leading to a specialisation of eqn. (2.20) by our Gaussian approximation to

$$\chi(t) = -\beta\Theta(t)\dot{C}(t)\,. \tag{2.22}$$

This assumption means treating the fluctuations as a Gaussian field in space. However of course, although so in surprisingly many situations, it is not always justified and more generally we should expect the susceptibility to be distributed in a more complicated way than as given in eqn. (2.21). But we leave these cases aside for the immediate purposes. The first thing we remember about $\chi(t)$ is that it satisfies causality, $\chi(t<0)=0$. This makes it possible to define its Laplace transform

$$\chi(z) = \int_0^\infty \mathrm{d}t\,\chi(t)\mathrm{e}^{-st} \tag{2.23}$$

which, as a function of the complex argument $z \in \mathbb{C}$ is analytic in the positive half complex plane, as the integral only converges for $\mathrm{Re}\,s > 0$ (assuming $\chi(t)$ does not grow exponentially). However, it will turn out to be more useful to work with a slightly modified Laplace transform, which corresponds to a rotation of eqn. (2.23) in the complex plane. We define

$$\chi(z) = \int_0^t \mathrm{d}t\,\chi(t)\mathrm{e}^{izt} \tag{2.24}$$

which is now analytic in the upper half complex plane, i.e. for $\mathrm{Im}\,z > 0$. From eqn. (2.22) it follows that

$$\begin{aligned}\chi(z) &= -\beta\int_0^\infty \mathrm{d}t\,\dot{C}(t)\mathrm{e}^{izt} = -\beta\int_0^\infty \mathrm{d}t\int_{-\infty}^\infty \frac{\mathrm{d}\omega}{2\pi}\,i\omega C(\omega)\mathrm{e}^{i(z+\omega)t}\\ &= \beta\int_{-\infty}^\infty \frac{\mathrm{d}\omega}{2\pi}\,\frac{\omega C(\omega)}{z+\omega}\,,\end{aligned} \tag{2.25}$$

where $C(t)$ has been expressed by its Fourier transform $C(\omega)$. This relation can be seen as a *dispersion relation* for the susceptibility. We can regard $\chi(z)$ as the analytic continuation of the Fourier transform $\chi(\omega)$ to the upper half complex plane and write

$$\lim_{\epsilon\to 0^+}\chi(\omega+i\epsilon) = \chi(\omega)\,. \tag{2.26}$$

Using this in eqn. (2.25) gives

$$\begin{aligned}\chi(\omega) &= \lim_{\epsilon\to 0^+}\beta\int_{-\infty}^{+\infty}\frac{\mathrm{d}\omega'}{2\pi}\,\frac{\omega' C(\omega')}{\omega+\omega'+i\epsilon}\\ &= \mathrm{PV}\left\{\beta\int_{-\infty}^{+\infty}\frac{\mathrm{d}\omega'}{2\pi}\,\frac{\omega' C(\omega')}{\omega+\omega'+i\epsilon}\right\} + \beta\frac{i\pi}{2\pi}(-\omega)C(-\omega)\end{aligned} \tag{2.27}$$

where PV denotes the Cauchy principle value of the integral, which is a real number. We also know that $C(t)$ is an even and real function so that its Fourier transform $C(\omega)$ must be real. This lets us conclude that

$$\mathrm{Im}\,\chi(\omega) = -\frac{\beta}{2}\,\omega C(\omega)\,. \tag{2.28}$$

With $C(\omega)$ being the Fourier transform of $\langle\phi(t)\phi(0)\rangle_0$, the right hand side of this result is clearly a measure for the equilibrium fluctuations. The imaginary part of the susceptibility can be shown generally to be responsible for dissipation in a system. A rigorous discussion of this can be found in [10]. For our purposes, it will be enough to give only an intuitive understanding of this fact by the following elementary argument.

Consider an external force of the simple form $j(t) = j_\omega \cos(\omega t)$ and write the susceptibility $\chi(t) = \mathrm{Re}\chi(t) + i\,\mathrm{Im}\chi(t) \equiv \chi_1(t) + i\,\chi_2(t)$. We know that $\chi_1(\omega)$ must be even. Due to eqn. (2.28) however, $\chi_2(\omega)$ will be odd. Further, the Fourier transformed external force will be $j(\omega') = \pi f_\omega[\delta(\omega+\omega') + \delta(\omega-\omega')]$. Bringing all this together, we then have according to eqn. (2.17):

$$\begin{aligned}\langle\delta\phi(t)\rangle &= \int \mathrm{d}t'\,\chi(t-t')j(t') = \int \frac{\mathrm{d}\omega'}{2\pi}\,\chi(\omega')j(\omega')\mathrm{e}^{i\omega' t} \\ &= \frac{1}{2}f_\omega\Big(\chi(-\omega)\mathrm{e}^{-i\omega t} + \chi(\omega)\mathrm{e}^{+i\omega t}\Big) = f_\omega\Big(\chi_1(\omega)\cos\omega t - \chi_2(\omega)\sin\omega t\Big) \\ &= \Big(\chi_1(\omega) + \chi_2(\omega)\omega^{-1}\partial_t\Big)j(t) \qquad (2.29)\end{aligned}$$

Hence we see for this example that that part of the response being out of phase with the driving force, and thus corresponding to dissipative contributions proportional to $\partial_t j$, is governed by $\mathrm{Im}\,\chi(\omega)$. With this argument in mind, we can now really appreciate the content of eqn. (2.28), which is the classical version of the *fluctuation-dissipation theorem*. We derived it in the approximation that the fluctuations in the field are uncorrelated in space but in fact it can be generalised by modifying the ansatz from eqn. (2.21). The statement that stays unaltered is that, for small perturbations around the equilibrium, the fluctuations in the field are the immediate cause for dissipative effects. As one would expect, this relationship is amplified for higher temperautures β^{-1}. Also, the relation is weighted by frequency, which means that correlations at higher frequencies give rise to more losses than those at low frequencies.

2.2 Homotopy classes

In the preceding section it has been seen how causality limits the time it takes a system to react on an external source of excitation, but in the same way also the time it needs to relax back to equilbrium. Hence the conclusion must be that if a critical point is passed too quickly, then it is possible for sufficiently distinct regions to remain causally unrelated for an amount of time that has been long enough for them to choose their respective groundstates independently, giving rise to the formation of domain structures. Before the next section will provide a more detailed reasoning for this in terms of the Kibble-Zurek mechanism, it will now be shown how the different possible domain structures are categorised purely by their topological conditions.

When discussing the spontaneous breaking of a continuous symmetry group G to some subgroup H, we identified the degenerate set of broken vacuum states as the coset $\mathcal{M}_0 = G/H$ and named it the vacuum manifold. In 1995, Kléman could show [11] that the conditions on the existence and shape of toplogical defects all follow from the structure of $\mathcal{M}_0$ and in particular from its *homotopy classes*.

Consider first the simple case of $\mathcal{M}_0$ being a disc with a hole cut out of it. Starting from any point $\phi_0 \in \mathcal{M}_0$, there will be different kinds of closed loops, some going

around the hole and some not. If we identify those loops with each other that can be deformed into another in a continuous way, i.e. without crossing the hole and thus leaving $\mathcal{M}_0$, then there will be a clear classification of loops by the number of times they wrap around the hole. This number is called the *winding number*. Loops that can be deformed into each other in the allowed way are called *homotopic* and together form a homotopy class. Note that this classification does not depend on the point ϕ_0 we chose as the starting and ending point of the loops. A further observation is that the different homotopy classes as a whole own a group structure. This can be seen in our simple example by taking the group product to be the composition of loops. Then, every loop will have an inverse which corresponds to the same loop but with opposite orientation (i.e. reversely parametrised), while the identity is given by the homotopy class corresponding to zero winding number, i.e. containing those loops that do not go around the hole. If the classes comprise closed loops, the arising group is denoted by $\pi_1(\mathcal{M}_0)$ and called the *fundamental group*. From our characterisation by the winding number we note that if $\mathcal{M}_0$ has the form of a disc with a whole cut out, then $\pi_1(\mathcal{M}_0) = \mathbb{Z}$.

The notion of homotopy can be generalised from closed loops to other and higher dimensional closed surfaces which then give other homotopy groups. The meaning of a homotopy class simply generalises: For a closed n-dimensional hypersurface $\Sigma^{(n)}$ containing ϕ_0, the corresponding homotopy class will comprise all other closed n-dimensional hypersurfaces $\Sigma^{(n)'}$ that also contain ϕ_0 and can continuously be deformed into $\Sigma^{(n)}$.

One example is the *second* homotopy group $\pi_2(\mathcal{M}_0)$. Its elements are the homotopy classes of maps from the two-sphere S^2 into $\mathcal{M}_0$. $\pi_0(\mathcal{M}_0)$ consists of classes of maps from the S^0 to $\mathcal{M}_0$. As S^0 only includes two points (it is the boundary of a line segment), $\pi_0(\mathcal{M}_0)$ effectively counts the number of disconnected pieces in $\mathcal{M}_0$.

It belongs to the immediate conclusions of these observations that domain walls can only exist when the vacuum manifold is disconnected, i.e. $\pi_0(\mathcal{M}_0)$ is not the trivial group. If $\mathcal{M}_0$ is not simply connected, which means there are non-shrinkable loops as described above and so $\pi_1(\mathcal{M}_0)$ is not trivial, then *strings* can form. Further, monopoles can exist if $\pi_2(\mathcal{M}_0)$ is non-trivial.

For our example of a broken $U(1)$ symmetry, the stability group was trivial and so we found $\mathcal{M}_0 = U(1)$. The circle $U(1) \simeq SO(2)$ is connected but not *simply* connected and so we expect strings to appear from such a transition. As we will observe later, they become manifest in a continuously varying phase along the circle in space.

From the analysis of homotopy groups follow further major insight to all of which we may only refer here. Much of them rely on the simplification that the vacuum manifold can be written as a coset. In particular, stability of the various topological structures is addressed but also the means by which composite defects can emerge from sequences of phase transitions.

2.3 The Kibble-Zurek mechanism

Zurek and Kibble (Z&K) were the first to develop a possible scenario of how continuous phase transitions might be realised in systems that cannot be approximated by the standard framework of equilibrium statistical mechanics, which could be the early universe or condensed matter systems. For the original work, see [12], [13], [14]. The

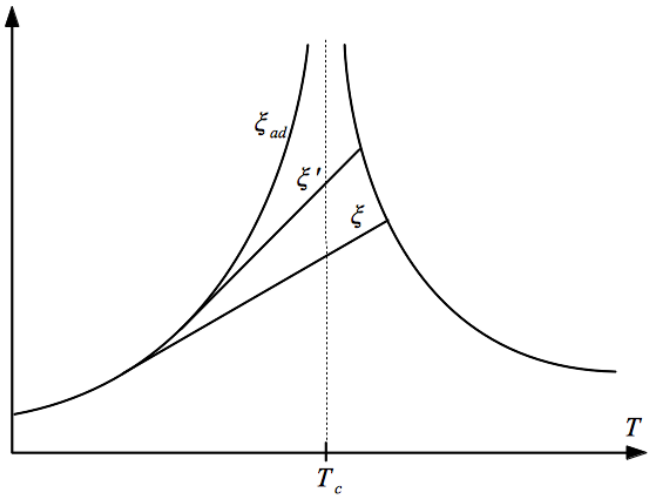

Figure 2.1: While the adiabatic correlation length ξ_{ad} diverges at the critical point, causality prevents the true correlation length to do so. Assuming it grows as fast as possible, its shape will be given by ξ in relativistic scenarios, or ξ' if the causal speed is smaller than the speed of light.

basic argument begins with realising that in real systems the correlation length ξ will stay finite, deviating from the equilibrium value in the critical region. The prediction of a diverging correlation length like in eqn. (1.107) relied on adiabaticity. But in reality, the temperature cannot change infinitely slowly. Moreover, the speed at which correlations propagate in a system must be bound by the relevant finite causal speed in the respective medium, which could be the speed of light or sound. Thus in essence, it is causality that puts the major bounds on the validity of an equilibrium description of phase transitions. In conclusion, there must be a maximum correlation length $\hat{\xi}$. This has fundamental consequences for the realisation of symmetry breaking in the order parameter. If different regions in a system cannot communicate changes in the order parameter fast enough to keep up with the speed at which the external conditions change, then it becomes inevitable that spatial domains form, of which each will minimise the energy, but will correspond to a different point on the vacuum manifold $\mathcal{M}_0$ and hence show a different value of the order parameter. While the *type* of defects that can form is completely defined topologically, their spatial distribution is random and can even be subject to further evolution governed by new dynamics appearing after the transition. The prediction of their *density* however can be attempted and a first handle is provided by the approach of Z&K. The prediction of defect densities is of great interest in the cosmological setting, where the hope is to gain a better understanding for the role of strings in the early universe. Due to the fact that the qualitative description is identical, there exist the great hope that experiments with condensed matter systems might yield insights into the era of the universe where the known forces were unified.

Imagining the change in temperature of a system given by a function $T(t)$ in time

with $T(0) = T_c$, we can write

$$\hat{\xi} = \xi_{\text{eq}}(T(\hat{t})) \tag{2.30}$$

with ξ_{eq} being the equilibrium correlation length with predicted pole at $T = T_c$. The question then becomes what the time $\hat{t}$ is, or equivalently, when the real dynamics diverge from the equilibrium ones. First it is assumed that T changes at a characteristic scale τ_q, which is called the quenchtime, and can be defined to be the rate of change in temperature at the critical point:

$$\tau_q^{-1} := -T_c \frac{\mathrm{d}T}{\mathrm{d}t}\bigg|_{T=T_c} \tag{2.31}$$

A linear quench would mean $T_{\text{lin}}(t) = T_c(1 - t/\tau_q)$ but other quench forms are conceivable and their relevance has to be discussed. An upper bound on $\hat{t}$ is given by the time $\hat{t}_> > \hat{t}$ at which the growth of the equilibrium correlation length exceeds the relevant causal speed c in the system

$$\frac{\mathrm{d}\xi_{\text{eq}}}{\mathrm{d}t}\bigg|_{t=\hat{t}_>} = c\,. \tag{2.32}$$

$\hat{t}_>$ actually becomes a good estimate for $\hat{t}$ in the early universe but in condensed matter systems the dynamics of the order parameter significantly refine the constraints merely inferred from causality. One therefore refers to the relaxation time τ of the system as a second time scale, for which the equilibrium value is known to obey a similar diverging power law as the correlation length:

$$\tau_{\text{eq}}(t) = \frac{\tau_0}{\vartheta(t)^{\nu z}} \tag{2.33}$$

The reduced temperature is her for convenience taken to be $\vartheta(t) = |T(t) - T_c|/T_c$, and τ_0 is the relaxation time far from the critical point. The true value τ stays finite but will still grow faster than ϑ. Z&K suggest to approximate $\hat{t}$ as the time when the relaxation length first grows above the time left to reach the critical point. This instant is referred to as the *freeze-out* time. At $\hat{t}$, it is still reasonable to approximate $\tau \simeq \tau_{\text{eq}}$ and so we can set

$$-\hat{t} \simeq \frac{\tau_0}{\vartheta(\hat{t})^{\nu z}} \simeq \frac{\tau_0}{(\hat{t}/\tau_q)^{\nu z}} \tag{2.34}$$

At the same time, the definition of the quenchtime can be exploited,

$$-\hat{t} \simeq \frac{\vartheta}{\mathrm{d}\vartheta/\mathrm{d}t}\bigg|_{t=\hat{t}}, \tag{2.35}$$

so that an estimate for the dependence of $\hat{t}$ on the quenchtime is possible as

$$\hat{t} \approx (\tau_0 \tau_q^{z\nu})^{\frac{1}{1+z\nu}}\,. \tag{2.36}$$

We assumed $\vartheta(\hat{t}) \simeq -\hat{t}/\tau_q$ and by combining this with eqn. (2.36), the correlation length at $\hat{t}$ will be

$$\xi(T(\hat{t})) = \xi_0 \left(\frac{\tau_q}{\tau_0}\right)^{\frac{\nu}{1+z\nu}} \tag{2.37}$$

with $\xi_0 = \xi_{\rm eq}(t \ll \hat{t})$. Both ξ_0 and τ_0 are parameters specific to a particular system and are often only determined by experiment. For short enough quenchtimes, the time spent in the vicinity of T_c is small enough to assume $\xi(T(\hat{t})) = \xi(T(-\hat{t}))$, which is known as the *impulse approximation*. In this case, the domains will be essentially set immediately after passing through the critical point and their typical seperation can be well approximated by the correlation length $\xi(\hat{t})$ at freeze-out. This is especially true when temperatures are small enough to prevent thermal fluctuations from changing the order parameter value for whole domains. If this is not the case, then a second length scale must be introduced, which will modify the result in eqn. (2.37) and is defined by the correlation length at the time when temperatures have fallen far enough to meet the above condition (c. f. [13]). Our concern however is the condensed matter side where we can rely on eqn. (2.37). In a d-dimensional system with characteristic linear length L, the Z&K prediction for the behaviour of the final defect density resulting from a quench is then given by

$$n_D \propto \frac{L^d}{\xi(T(\hat{t}))} \propto \tau_q^{-\sigma} \tag{2.38}$$

where we have renamed $\sigma := \frac{\nu}{1+z\nu}$.

2.4 Departure from scaling

While the Kibble-Zurek picture tries in some extent to convey the scaling behaviour from equilbrium transitions to the non-equilbrium situation, in the following will be shown that this cannot be true for all circumstances. Oriented along [15], the analysis is conducted for the case of a generic real scalar field theory in 1+1 dimensions and applies directly to the $\mathbb{Z}_2$ breaking case. Nevertheless, similar considerations are found to be applicable to the $U(1)$ case [16], and are expected to also be important for the $\mathbb{Z}$ breaking in Josephson Junctions.

In order to estimate the final defect density it is sufficient to start the observations in the broken phase, so that the field $\phi(x,t)$ faces a potential

$$V(\phi) = -\frac{\mu^2}{2}\phi^2 + \frac{\lambda}{4}\phi^4 \tag{2.39}$$

with *positive* μ. At any time t in the evolution, $\phi(x,t)$ corresponds to a certain configuration $\Phi(x)$ in space for which the equilibrium values lie at the two minima of V. Because none of them is preferred, at late times $\Phi(x)$ will exhibit a domain structure in which a transition between one potential minimum to the other must be accompanied by crossing $\Phi = 0$. This type of domain wall is called a *kink* when $\Phi'(x) > 0$ at the transition and an *antikink* when $\Phi'(x) < 0$. There are therefore two different relevant quantities: The total number of kinks plus antikinks and the *topological* number of kinks minus antikinks. Enumerating the zeroes of Φ at a given time by $x = x_1, x_2, ...$ the corresponding densities are, respectively,

$$\bar{\rho}(x) = \sum_i \delta(x - x_i) \tag{2.40}$$

and

$$\rho(x) = \sum_i \sigma_i \delta(x - x_i) \tag{2.41}$$

with $\sigma_i = \text{sign}(\Phi'(x_i))$. In terms of Φ, these translate into

$$\bar{\rho}(x) = \delta[\Phi(x)]\,|\Phi'(x)| \tag{2.42}$$

and

$$\rho(x) = \delta[\Phi(x)]\Phi'(x)\,. \tag{2.43}$$

To each configuration $\Phi(x)$ at a time t, we can ascribe a probability $p_t[\Phi]$ that it will correspond to the true realisation of $\phi(x,t)$. The ensemble average $\langle \mathcal{O}[\Phi]\rangle_t$ of a quantity at t then means weighting by these probabilities. If the broken symmetry is exact, kinks and antikinks are expected to appear with equal probabilities so that

$$\langle \rho(x)\rangle_t = 0\,. \tag{2.44}$$

Their total number however will be non-zero and obey

$$\begin{aligned} \bar{n}(t) &= \langle \bar{\rho}(x)\rangle_t \\ &= \int \mathcal{D}\Phi\, p_t[\Phi]\delta[\Phi(x)]\,|\Phi'(x)| \;>\; 0\,. \end{aligned} \tag{2.45}$$

How the zeroes of the field distribute is best described by the correlation function for the topological density

$$\begin{aligned} \tilde{C}(x;\,t) &= \langle \rho(x)\rho(0)\rangle_t \\ &= \int \mathcal{D}\Phi\, p_t[\Phi]\;\delta[\Phi(x)]\;\delta[\Phi(0)]\;\Phi'(x)\,\Phi'(0)\,. \end{aligned} \tag{2.46}$$

Note that defining a corresponding quantity for $\bar{\rho}(x)$ will not be as useful because it does not capture the fact that a kink can only be followed by an antikink and vice versa. In this sense, $\rho(x)$ must be considered the more natural quantity. We evaluate $C(x;\,t)$ by taking from eqns. (2.40) and (2.41) that

$$\rho(x)\rho(y) = \bar{\rho}(x)\delta(x-y) + \sum_{i\neq j} \sigma_i\sigma_j \delta(x-x_i)\delta(y-y_i) \tag{2.47}$$

and defining

$$C(x-y;\,t) := \Big\langle \sum_{i\neq j} \sigma_i\sigma_j \delta(x-x_i)\delta(y-y_i)\Big\rangle_t \tag{2.48}$$

so that it follows:

$$\tilde{C}(x;\,t) = \bar{n}(t)\delta(x) + C(x;t)\,. \tag{2.49}$$

The condition that the integral of $\tilde{C}(x;t)$ over the whole space must give zero can be thought of as charge conservation:

$$\int_{-\infty}^{+\infty} \mathrm{d}x\, \tilde{C}(x;t) = 0 \tag{2.50}$$

This constraint simply reflects the circumstance that kinks and antikinks appear with equal probability. Using it on eqn. (2.49) implies

$$\int_{-\infty}^{+\infty} \mathrm{d}x\, C(x;\, t) = -\bar{n}(t)\,, \tag{2.51}$$

which settles formally what could have been inferred already from eqns. (2.45) and (2.49): The density correlation function $\tilde{C}(x;\, t)$ splits into a strictly positive diagonal and a non-diagonal part that is largely negative.

On some finite interval $x \in [0, L]$ we find the *topological charge*

$$n_L = \int_0^L \mathrm{d}x\, \rho(x)\,, \tag{2.52}$$

which, in the case of a broken $\mathbb{Z}_2$-symmetry can only assume three values, namely $n_L \in \{-1, 0, 1\}$. By virtue of eqns. (2.49) and (2.51), its variance becomes

$$\begin{aligned}
(\Delta_t n_L)^2 &= \langle n_L^2 \rangle_t - \langle n_L \rangle_t^2 = \langle n_L^2 \rangle_t \\
&= \int_0^L \mathrm{d}x \int_0^L \mathrm{d}y\, \langle \rho(x)\rho(y) \rangle_t \\
&= L\bar{n}(t) + \int_0^L \mathrm{d}x \int_0^L \mathrm{d}y\, C(x-y;\, t) \\
&= -\int_{x<0}^{x>L} \mathrm{d}x \int_0^L \mathrm{d}y\, C(x-y;\, t)\,,
\end{aligned} \tag{2.53}$$

which due to vanishing average, is equal to the probability of the topological charge being either $+1$ or -1, or equivalently the probability that there is an odd number of zeroes in the interval $[0, L]$. As $C(x;\, t) = C(-x;\, t)$, we can rewrite eqn. (2.53) as

$$\begin{aligned}
(\Delta_t n_l)^2 &= -\int_0^L \mathrm{d}y \int_{-\infty}^0 \mathrm{d}x\, C(y-x;\, t) - \int_L^\infty \mathrm{d}x \int_0^L \mathrm{d}y\, C(x-y;\, t) \\
&= -\int_0^L \mathrm{d}y \int_{-\infty}^0 \mathrm{d}x\, C(y-x;\, t) + \int_0^\infty \mathrm{d}x \int_{-L}^0 \mathrm{d}y\, C(x-y;\, t)\,,
\end{aligned} \tag{2.54}$$

where in the second term both integration variables have been shifted by $-L$. Thus, the variance $(\Delta_t n_l)^2$ changes with L as follows:

$$\frac{\mathrm{d}}{\mathrm{d}L}(\Delta_t n_L)^2 = \frac{\mathrm{d}}{\mathrm{d}L}\Big[-\int_{-L}^L \mathrm{d}x\; C(x;\, t) + \text{const.}\Big] \tag{2.55}$$

with those terms suppressed as const. that are independent of L. Taking one further derivative results in a relation between correlations in the defect density and the variance of the topological charge:

$$\frac{\mathrm{d}^2}{\mathrm{d}L^2}(\Delta_t n_l)^2 = -2C(L;\, t) \tag{2.56}$$

Two extreme cases can be distinguished. For perfect correlation, the zeroes are located equidistantly with some seperation $\xi(t)$. Then $C(x;t)$ is a sum of delta functions with alternating sign while $(\Delta_t n_L)^2$ has saw-tooth shape. However, more interesting for the purposes of this work is the opposite limit of independent zeroes, Poisson-distributed with a mean distance of $\xi(t)$. In this case we expect that on average $L/(\xi(t)/2)$ zeroes will be found in the interval $[0, L]$ so that

$$(\Delta_t n_L)^2 = \langle n_L^2 \rangle_t = \mathrm{e}^{-2L/\xi(t)}/2 \tag{2.57}$$

and from eqn. (2.56) it follows

$$C(L;\, t) = -\mathrm{e}^{-2L/\xi(t)}/\xi(t)^2\,. \tag{2.58}$$

For large intervals $L \gg \xi(t)$, this tends to zero so that we can estimate $(\Delta_t n_L)^2 = \langle n_L^2 \rangle_t = \mathcal{O}(L/\xi)$, i.e. a linear dependence of the expected squared number of defects on the interval length. This results should also be valid for periodic boundary conditions as their effect will vanish in the limit of large L. On the other hand, if the interval we are interested in is as short as $L << \xi$, then we can expand $C(L;t)$ in powers of L/ξ and find $\langle n_L^2 \rangle_t \sim \mathcal{O}(L^2/\xi^2)$. However, in the case of small L, periodic boundary conditions must be expected to make this last estimate invalid.

3. Representatives: $\mathbb{Z}_2$, $\mathbb{Z}$ and $U(1)$

3.1 Emergence of criticality

3.1.1 Ion chains

One important test field for the study of non-linear dynamics in many models of statistical physics is provided by systems of equally charged ions that are spatially confined in Pauli or Penning traps [17] which, depending on their various architectures, generate suitable electromagnetic fields that can be described as effective potentials in which the ions distribute. Laser cooling is employed to extract kinetic energy from the ions and thus regulate the temperature of the system. While at high temperatures the ions are found to be in an unordered configuration, at sufficiently low temperatures they form Wigner-like crystals of which the shape is determined by the Coulomb interaction between the ions [18]. Importantly, during the last two decades it has been recognised that in response to a variation of the trapping potential, the trapped ion chains exhibit structural changes that can be described as non-equilibrium continuous phase transitions [19] and as such are subject to a comparison against the predictions of the Kibble-Zurek picture. In the following, only one-dimensional systems of this kind will be reviewed, for which crystalisation means that the ions settle in equidistant positions on a line, each of them well-described as being in some low-energy, only-vibrational state. Both linear and circular chain configurations are studied. While the critical behaviour is expected to be identical, each of them introduces distinct experimental challenges and in particular the actual realisation of the transition is different.

The study of linear chains is usually constrained to a relatively small number of ions, N being of the order of 10. This is due to density gradients that inevitably develop towards the centre of the chain where the axial trapping potential is lowest. Inhomogenieties like this gain importance with increasing chain length and quickly make the crystal model invalid. Usually, like recently done in [20], the structural transition is then induced by willingly increasing the axial while keeping constant the transverse confinement. At a critical point, the so augmented Coulomb repulsion between the ions leads to a break up of the linear to what is usually called a *zig-zag* structure — a configuration in which initially neighbouring ions oppose each other.

More suitable to study the behaviour of larger number of ions are circular chains that are preparable in multipole traps (e.g. [21], [22]) or storage rings (e.g. [23], [24]),

which constrain the trapping potential to the plane perpendicular to the axis and hence are capable of creating homogeneous chains much closer to the thermodynamic limit and admit the study of periodic boundary conditions. Circular chains assume a zig-zag structure when the transverse trapping potential is lowered below a critical value.

For both the linear and the circular chains the global form of the zig-zag configuration after the phase transition is determined by the shape of the transverse trapping potential.

If the transverse potential is strongly anisotropic, i.e. the confinement in one of the transverse directions can be neglected against the other, then the zig-zag structure is in fact a plane bordered by two chains which have emerged form the initial one, each consisting of $\sim N/2$ ions separated by $\sim 2a$ if the initial lattice constant was a. Defects are identified at lattice sites where this planar zig-zag order is broken.

If the transverse potential is rotationally symmetric around the chain axis, then the local zig-zag structure globally has to be seen not as a plane but as a double helix that will have inherited a number of twists from the transition. These are captured in a *winding number* that can be taken as a measure for the defect density.

While the case of an anisotropic transverse trapping potential can be viewed as an instance of spontaneous $\mathbb{Z}_2$ symmetry breaking, in the axisymmetric situation a $U(1)$ symmetry is being broken. These are precisely the two generic situations that we have encountered earlier when presenting the Ising model and Landau theory. In the rest of this section we will see how the description for a typical realisation of an ion chain [25] continues this correspondence by deriving for this representative system the equations that govern the dynamics of the order parameter for phase transitions in this universality class.

The typical potential U for a chain oriented along the x-axis and consisting of N ions, with mass m, charge q and coordinates $\mathbf{r}_i = \{x_i, y_i, z_i\}$ can be written most generally as

$$\bar{U} = \frac{m}{2}\sum_{i=1}^{N}(\omega_x^2 x_i^2 + \omega_y^2 y_i^2 + \omega_z^2 z_i^2) + \frac{1}{4\pi\epsilon_0}\,\frac{1}{2}\sum_{i,j=1}^{N}\frac{q^2}{|\mathbf{r}_i - \mathbf{r}_j|}\,, \tag{3.1}$$

when applying Gaussian cgs-units. While the second term accounts Coulomb potential of the configuration, the first term represents the common approximation that the trapping potential be harmonic in all of the three directions. For the purpose of the following analysis we will focus on circular chains and set $\omega_x = 0$. Also we will ignore the case of a weakly anisotropic transverse potential. The axisymmetric case is obtained by specifying only one transverse frequency $\omega := \sqrt{\omega_y^2 + \omega_z^2}$ so that we have

$$U = \frac{m}{2}\sum_{i=1}^{N}\omega^2(y_i^2 + z_i^2) + \frac{1}{2}\sum_{i,j=1}^{N}\frac{q^2}{|\mathbf{r}_i - \mathbf{r}_j|}\,. \tag{3.2}$$

From there we will finally be able to obtain the limit of strongly anisotropic trapping by setting either of the transverse direction y_i, z_i to zero. Solving for the ground state

configuration $\{\bar{\mathbf{r}}_i\}$ by setting

$$\frac{\partial U}{\partial \mathbf{r}_i}\Big|_{\mathbf{r}_i=\hat{\mathbf{r}}_i} \qquad \forall\, i \tag{3.3}$$

one finds [26] a critical frequency

$$\omega_c = \sqrt{\frac{7\zeta(3)}{2}}\,\omega_0\,, \tag{3.4}$$

where ζ denotes the Riemann zeta function and $\omega_0 = \sqrt{q^2/ma^3}$ is a characteristic frequency. While for $\omega > \omega_c$ the potential is minimised only by $y_i = z_i = 0\ \forall i$, when $\omega < \omega_c$ the ground state configuration has zig-zag shape. Note that it should be anticipated that condition eqn. (3.3) will not completely determine $\{\bar{\mathbf{r}}_i\}$ but instead give rise to a free parameter corresponding to a massless Goldstone mode. Because it is a real system (c.f. M in fig. 1.1.4), instabilities in the ion chain grow already at values of ω_t slightly above ω_c, also all others observable consequences of the precise mathematical description of phase transition in the thermodynamic limit will never be exactly present. But once having accepted the hypothesis that this structural change in the ion chains corresponds to a continuous, symmetry breaking phase transition one can at this point adopt a phenomenological point of view and apply Landau's effective continuum description to this one-dimensional problem as long as the corresponding order parameter, which we will in this context call $A(x)$, varies on scales much larger than the lattice spacing a. This condition is indeed satisfied when $A(x)$ is taken to describe the position of the ion chain measured from the x-axis, i.e. $A(x) = y + i\,z$. This is a valid choice of order parameter when the initial stable chain is taken to lie at $x = 0$, so that then the expectation value for $A(x)$ will change from zero to non-zero value during the transition. In the $\mathbb{Z}_2$ breaking case of strongly anistoropic transverse confinement A reduces to be real-valued, while for rotational symmetry it has to be complex in order to capture the $U(1)$ breaking. Then, the angle $\theta(x) := \arg A(x)$ gives the angular position of the chain at x. The precise analysis of this exact situation has been done already when introducing Landau theory.

A correct Lagrangian $L(A, A^*)$ should be reconcilable with the expected dynamics resulting from eqn. (3.2). Either by making a phenomenological ansatz for the energy of a particular configuration or simply by writing down the most general form for the Lagrangian of a complex scalar field and afterwards adjusting the parameters, one finds in the vicinity of the critical point [26]:

$$\begin{aligned} L(A, A^*) &= \int \mathrm{d}x\, \mathcal{L}\big(A(x,t), A^*(x,t)\big) \\ &= \frac{m}{a}\int \mathrm{d}x \left[\ |\partial_t A|^2 - h^2|\partial_x A|^2 - \delta|A|^2 - \frac{g}{2}|A|^4\ \right] \end{aligned} \tag{3.5}$$

with the first term being kinetic and all others corresponding to the (negative) potential, and where the (x,t) dependece has been suppressed. The equation of motion for A is

$$\begin{aligned} 0 &= \frac{\partial \mathcal{L}}{\partial A^*} - \sum_{\mu=t,x} \partial_\mu \frac{\partial \mathcal{L}}{\partial(\partial_\mu A^*)} \\ &= \frac{m}{a}\Big[-\big(\delta A + g|A|^2 A\big) - \big(\partial_t A - h^2\partial_x^2 A\big)\Big]\,, \end{aligned} \tag{3.6}$$

where $\delta = \omega_t^2 - \omega_c^2$ plays a role equivalent to that of the chemical potential in the discussion of Landau theory and h, g are some realisation-specific constants of which the precise value is not central to the following discussion. Eqn. (3.6) extremises the action $S = \int \mathrm{d}t L$, and thus so far we only describe an equilibrium situation. However, we know that fluctuations will be present and that they may have multiple causes. Internal sources can be of quantum or thermal nature. And among the many possible external influences that arise in an experiment will certainly at least be small variations in the trapping potential. With the justification that the fluctuations will be attributable to a variety of effects, one customarily makes the Gaussian approximation that was presented in sec. 2.1. And thus without making explicit reference to the details, one takes into account the Fluctuation-Dissipation theorem by adding two further terms to eqn. (3.6) – one that acts as a stochastic force term $\epsilon(x,t)$ and at the same time another one which implements dissipation of some intensity η into the system. According to eqn. (2.28), at a temperature T, in the Gaussian approximation their relation is given by

$$\left\langle \epsilon(x,t)\epsilon(x',t') \right\rangle_0 = 2\eta k_B T\, \delta(x-x')\delta(t-t') \tag{3.7}$$

where

$$\left\langle \epsilon(x,t) \right\rangle_0 = 0 \tag{3.8}$$

and the averages are taken in equilibrium, analogously to eqn. (2.3). Including fluctuations in A in this way, eqn. (3.6) becomes

$$\left[\partial_t^2 - h^2\partial_x^2 + \eta\partial_t + g|A(x,t)|^2 + \delta(t) \right] A(x,t) = \epsilon(x,t)\,, \tag{3.9}$$

where δ has been been made time-dependent to refer to a process in which a phase transition is imposed externally by tuning the trapping potential. An equation of this type is known in the literature as a *Langevin* equation. In strongly dissipative situations (large η) the relaxation of the systems happens on a time scale much larger than the scale at which fluctuations take place. In that case the second time derivative can effectively be neglected and one obtains instead a first order differential equation in time. Given an inital configuration, differential equations like (3.9) are usually considered impossible to solve analytically. An attempt to extract at least some information in terms of the critical exponents is given by the Kibble-Zurek approach. The numerical investigation in the last section of this work will address how far this is possible.

3.1.2 Superconductors

A microscopic explanation of superconductivity has been provided by Bardeen, Cooper and Schrieffer in 1957 [27]. Their fundamental insight was that in a solid below a critical temperature T_c, valence electrons with opposite momenta can form boundstates via interaction with the lattice phonons to give rise to bosonic quasiparticles. These *Cooper pairs* have twice the elementary charge and can condense in a single state. Ginzburg and Landau had been unaware of the underlying microscopic dynamics when, years before, they had already realised that near the critical point, the essential behaviour of superconductors can also be understood in terms of a single macroscopic

wavefuntion due to similar ideas as presented in sec. 1.2.1, but additionally respecting the dynamics of the electromagnetic gauge field. Gorkov then showed in 1959 that the Ginzburg-Landau theory is not merely phenomenological but can be derived in a limiting procedure from the microscopically underlying BCS theory of superconduction. It is this what justifies a description of the superconducting phase transition in terms of the Ginzburg-Landau theory and in fact, the macroscopic wavefunction has the role of the corresponding order parameter. Its form is

$$\Psi(\mathbf{r},t) = \sqrt{n(\mathbf{r},t)}\mathrm{e}^{i\phi(\mathbf{r},t)} \tag{3.10}$$

where the squared modulus equals the Cooper pair density $n(\mathbf{r},t)$, i.e. the fraction of electrons that has condensed into the Cooper pair state. When a superconductor cools down across its critical temperature, this number rises from 0 to 1. For type-II superconductors, the transition is continuous and it is induced by the spontaneous $U(1)$ gauge symmetry breaking by which the vector potential loses its local $U(1)$ invariance. Once phrased like this, the Meißner effect, which is the expulsion of magnetic flux from the interior of a superconductor, does not appear as a phenomenon separated from the one of vanishing electric resistance. Together they are merely the two sides of the same coin signifying the breakdown of electromagnetism's local $U(1)$ invariance. Each phase $\phi(\mathbf{r},t)$ in (3.10) corresponds to one choice of gauge.

In superconducting rings, an additional global $U(1)$ symmetry arises due to the requirement of a single-valued order parameter which, when being spontaneously broken, can give rise to flux trapping during non-equilibrium transitions. Hence, annular configurations of superconductors provide a further test-field for the predictions of Z&K in the laboratory. For thin rings, the order parameter can be viewed to effectively vary in only one dimension, where magnetic fields become non-dynamical. Then, under idealised experimental conditions, not only the same critical behaviour has to be expected from annular superconductors as for ion chains trapped in an isotropic transverse potential as described above. But in fact, these two experimental situations will be captured to a good approximation by the *same theory* – Ψ will take the same role as A in eqn. (3.9):

$$\Big[\,\partial_t^2 - h^2\partial_x^2 + \eta\partial_t + gn(x,t) + \delta(t)\,\Big]\,\Psi(x,t) = \epsilon(x,t)\,. \tag{3.11}$$

It is a remarkable fact that at the same time, there exist situations in which Ψ is sufficiently understood by ordinary quantum mechanics. A prominent example is given by Josephson Junctions.

3.1.3 Josephson Junctions

When two superconductors are linked by a small region of vanishing superconductivity, there might still be a supercurrent observable between them. If this is the case, then the configuration is called a Josephson (Tunnel) Junction, due to Josephson who first described the responsible mechanism in 1962. The connecting barrier can be understood as a *weak link* and might be an insulator, a regular conductor or a purely geometrical obstruction. Irrespective of the realisation, very similar equations hold. It will become clear that the Josephson effect is a *macroscopic quantum phenomenon* and Josephson Junctions can have considerable spatial extent, at the micrometer

scale. It might thus not surprise that their common description borrows the notion of the macroscopic order parameter (3.10). But here, $\Psi(\mathbf{r},t)$ can be treated as an ordinary quantum mechanical wavefunction of a single particle obeying the Schrödinger equation

$$i\hbar\frac{\partial\Psi}{\partial t}(\mathbf{r},t) = H\Psi(\mathbf{r},t) \tag{3.12}$$

in the presence of an electromagnetic field, with the Hamiltonian

$$H = (-i\hbar\nabla + e\mathbf{A})^2/2m - e\Phi\,, \tag{3.13}$$

m and e being electron mass and charge. $\mathbf{A}$ and Φ are vector and scalar potential, transforming together with Ψ as

$$\begin{aligned}\Psi &\longmapsto \Psi \mathrm{e}^{i\chi}\\ \mathbf{A} &\longmapsto \mathbf{A} + \frac{1}{e}\nabla\chi\\ \Phi &\longmapsto \Phi - \frac{1}{e}\frac{\partial\chi}{\partial t}\,.\end{aligned} \tag{3.14}$$

Independent of the gauge remains the current density $\mathbf{j}$ that flows in the superconductor and which is given by

$$\mathbf{j}(\mathbf{r},t) = \frac{ne}{m}\left(\hbar\nabla\phi(\mathbf{r},t) - 2e\mathbf{A}(\mathbf{r},t)\right) \tag{3.15}$$

where e and m are electron charge and mass and $\mathbf{A}(\mathbf{r},t)$ is the gauge field. This form can be derived from the Lagrangian formulation of field theory or, even simpler, by considering the continuity equation

$$\nabla\cdot\mathbf{j} + \frac{\partial n}{\partial t} = 0 \tag{3.16}$$

together with the Schrödinger equation.

We shall not overuse this quantum mechanical viewpoint because the focus of this work lies on classical effects in phase transitions. Nevertheless, it provides immediate access to an understanding of Josephson Junctions.

In order to investigate the Josephson effect, we consider two superconductors, with wavefunctions $\Psi_1 = \sqrt{n_1}\mathrm{e}^{\phi_1}$ and $\Psi_2 = \sqrt{n_2}\mathrm{e}^{\phi_2}$, separated by a distance d. As d decreases and reaches the nm-scale, the flow of ordinary electronic current will be observed. But if the separation decreases even further ($d < 3\,\mathrm{nm}$ [28]) then Ψ_1 and Ψ_2 have an overlap and a flow of supercurrent, i.e. of Cooper pairs can be registered. Feynman's approach to a quantitative description [29] assumes a linear coupling between the two Schrödinger equations and, after simple algebraic manipulation and treating real and imaginary parts separately, arrives at the *Josephson equations*:

$$j = j_0\sin(\varphi) \tag{3.17}$$

$$\frac{\mathrm{d}\varphi}{\mathrm{d}t} = 2eV/\hbar \tag{3.18}$$

The first relation states how the current density $j = |\mathbf{j}|$ across the junction depends on the *gauge independent phase difference*

$$\varphi = \phi_2 - \phi_1 - \frac{2e}{\hbar} \int_1^2 \mathrm{d}\mathbf{r} \cdot \mathbf{A} \,. \tag{3.19}$$

It is also known as the DC Josephson equation, as opposed to the second, AC Josephson equation which relates the rate of change in φ to the voltage V applied to the junction. The characteristic quantity j_0 is proportional to the coupling strength K between the superconductors and the Cooper pair density in the vicinity of the Josephson junction n_0:

$$j_0 = 2Kn_0/\hbar \tag{3.20}$$

It has to be stressed that the Josephson equations only capture the effects caused by Cooper pair tunneling through the junction. Geometrical effects as well as the contribution $\hat{\mathbf{j}}$ coming from single electron flow need to be considered separately. An expression for the full current

$$\mathbf{J} = \mathbf{j} + \hat{\mathbf{j}} \tag{3.21}$$

is derived in [30] where in conclusion the expression for the overall current density J across the junction takes the form

$$J = J_0 \sin\varphi + \left(\frac{1}{R_0(V)} + \frac{1}{R_1(V)} \cos\varphi \right) V \,. \tag{3.22}$$

The first term originates from the tunnelling of Cooper pairs, whereas the second and third terms take into account classical and quantum contributions respectively, $R_0(V)$ and $R_1(V)$ being voltage dependent parameters specific to geometry and material. The aim now is to find out about the full dynamics of φ throughout the barrier. The presentation below is largely oriented along [28].
We first consider a typical geometry, as depicted in fig. **??**. The two superconductors lie in the (x, y) plane. The insulator between them is taken to be of rectangular geometry with side lengths (L_x, L_y, L_z) in the three spatial dimensions. Furthermore, now we allow for an external magnetic field $\mathbf{H} \perp \hat{\mathbf{z}}$ to be applied in the junction plane, which will decay exponentially from the surface towards the bulk of the superconductors, on a length scale given by the *London penetration depth* $\lambda_{L,i}\,,\ i = 1, 2$. This is also where the supercurrents sit. We then define the distance characterising the thickness of the Josephson Junction to be $d = L_z + \lambda_1 + \lambda_2$. Taking an appropriate contour for the integration of (3.15) (see fig. **??**) and assuming $L_z/\lambda_i \ll 1$ the gradient of the phase difference becomes (in Gaussian cgs-units)

$$\nabla\varphi = \frac{2ed}{\hbar} \mathbf{H} \times \hat{\mathbf{z}} \,. \tag{3.23}$$

The junction is a non-superconducting area, where we can invoke Maxwell's equations. Ampère's law reads

$$\nabla \times \mathbf{H} = \hat{\mathbf{j}} + \frac{\partial \mathbf{D}}{\partial t} \tag{3.24}$$

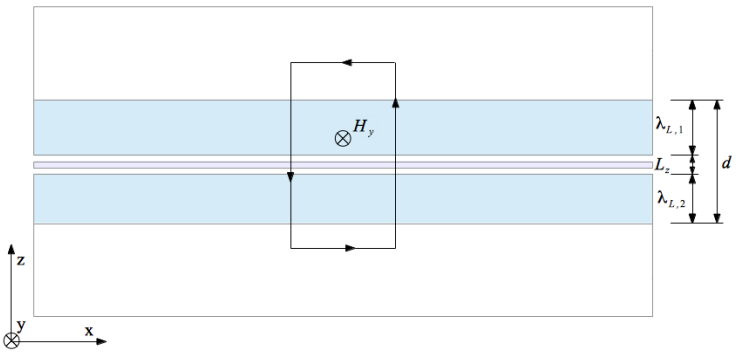

Figure 3.1: Schematic view on a Josephson Junction and the integration path to derive **H**- dependence of φ.

where in a preliminary approximation the low frequency limit $\frac{\partial \mathbf{D}}{\partial t} \approx 0$ will be sufficient. Further assuming Ohm's law with isotropic electrical resistance R in the junction region, i.e. $\mathbf{E} = R\hat{\mathbf{j}}$, it follows that

$$\mathbf{E} = R\,\nabla \times \mathbf{H}\ . \tag{3.25}$$

Taking the divergence on both sides, we realise that $\nabla \cdot \mathbf{E} = 0$ in the junction, as it should be because $(\nabla \cdot \nabla \times ...) \equiv 0$. But we can use this tautology by specifying $\mathbf{H} = (H_x, H_y, 0)$ as proposed above and thus extracting

$$\frac{\partial E_z}{\partial z} = -R\left(\frac{\partial^2 H_y}{\partial z \partial x} - \frac{\partial^2 H_x}{\partial z \partial y}\right) \tag{3.26}$$

or, after integration,

$$E_z = -\frac{U(t,x,y)}{L_z} + R\left(\frac{\partial H_y}{\partial x} - \frac{\partial H_x}{\partial y}\right) \tag{3.27}$$

with a z-independent function U. Now the crudity of the low frequency limit becomes obvious – neither V nor **H** are in principle constrained in their time behaviour. At best, **H** might be arranged for to vary slowly in time under experimental conditions. Treating any results from here on with precaution, we insert the last equation back into (3.24) to obtain

$$J_z = \left(1 + \epsilon R \frac{\partial}{\partial t}\right)\left(\frac{\partial^2 H_y}{\partial z \partial x} - \frac{\partial^2 H_x}{\partial z \partial y}\right) - \frac{\epsilon}{L_z}\frac{\partial V}{\partial t}\ , \tag{3.28}$$

which has to be equated to (3.22). Recalling (3.23) and defining

$$\lambda_J = \frac{1}{\sqrt{2edJ_0}} \tag{3.29}$$

$$c_S = \sqrt{\frac{L_z}{\epsilon d}} \tag{3.30}$$

this leads to

$$\left(\left[1+\epsilon R\frac{\partial}{\partial t}\right]\left[\frac{\partial^2}{\partial x^2}+\frac{\partial^2}{\partial y^2}\right]-\left[\frac{1}{R_0}+\frac{\cos\varphi}{R_1}\right]d\frac{\partial}{\partial t}-\frac{1}{c_s^2}\frac{\partial^2}{\partial t^2}\right)\varphi=\frac{1}{\lambda_J}\sin\varphi\ . \tag{3.31}$$

The Josephson coherence length λ_J and the *Swihart velocity* c_S together yield a characteristic time scale at which the dynamics happen. This *plasma frequency* is

$$\Omega=\frac{c_S}{\lambda_J}\ . \tag{3.32}$$

Rescaling time and space with respect to Ω and λ_J, and introducing the three dimensionless parameters

$$\alpha=\frac{L_z}{\epsilon\omega} \tag{3.33}$$

$$\beta=\epsilon R\Omega \tag{3.34}$$

$$\kappa=\frac{R_0}{R_1}\ , \tag{3.35}$$

we finally arrive at

$$\Box\varphi+\beta\Delta\dot{\varphi}-\alpha(1+\kappa\cos\varphi)\dot{\varphi}=\sin\varphi\,, \tag{3.36}$$

where $\dot{\varphi}=\partial\varphi/\partial t$ and

$$\Box=-\frac{\partial^2}{\partial t^2}+\Delta \tag{3.37}$$

$$\Delta=\frac{\partial^2}{\partial x^2}+\frac{\partial^2}{\partial y^2}\ . \tag{3.38}$$

Our result is the *Perturbed Sine-Gordon Equation* (PSGE) and it approximises the dynamics of the electron plasma in the junction in terms of the gauge invariant phase difference between the order parameters of the two adjacent superconductors, in the presence of an external magnetic field and with the given geometry. It incorporates a $\mathbb{Z}$-symmetry, which is seen from the fact that it is invariant under a constant shift of ϕ by any multiple of 2π. Without dissipation, the PSGE reduces to the Sine-Gordon equation

$$\Box\varphi=\sin\varphi \tag{3.39}$$

which differs from the Klein-Gordon-equation (KGE) for a relativistic real scalar field, $\Box\varphi=0$, only in the additonal sine-term, thus giving reason to the similarity yet difference in name. It has to be stressed that the SGE is still a Lorentz invariant equation, the speed of light in vacuum only replaced by the Swihart velocity c_S.

But of course, the PSGE involves a dissipative term, which had to be expected as soon as we included usual electrical conductance. In fact, by only thinking about a Josephson junction, we made the premise of broken superconductivity. Least easily understood remains the mixed derivative term $\sim\Delta\dot{\varphi}$, which further adds to the complexity of the dynamics of φ. Some first insights are obtained by considering the

limiting cases.

The static solution φ_0 of the PSGE is easily seen to obey

$$\Delta\varphi_0 = \sin\varphi_0\,, \tag{3.40}$$

which for small phase differences $\varphi \ll 1$ and after restoring units has exponentials as the fundamental solution,

$$\varphi_0(x,y) \propto \mathrm{e}^{\frac{+(x\pm y)}{\sqrt{2}\lambda_J}}\,,\ \mathrm{e}^{\frac{-(x\pm y)}{\sqrt{2}\lambda_J}} \tag{3.41}$$

with four coefficients determined via (3.23) by the derivatives of $\mathbf{H}$ at the boundary of the junction.

A second case is immediately accessible. This is for small junctions, i.e. $L_i \ll \lambda_J$, φ may be approximated by a constant in space which oscillates in time, as realised after restoring units, with a frequency ω_J

$$\frac{\partial^2\varphi}{\partial t^2} + \omega_J \sin\varphi = 0\ . \tag{3.42}$$

For small amplitudes as considered above already, a harmonic oscillator is recovered, with solutions of the form (3.41) but with imaginary exponents.

The system of immediate interest to us is a long and narrow Josephson Junction, which can effectively be treated as one- dimensional in space. As already seen in the case of ionic crystals, one accomodates for fluctuations in φ by adding a random force term $\epsilon(x,t)$ to the equations of motion, which is supposed to approximately obey eqns. (3.7) and (3.8). Furthermore, one usually neglects those terms in the PSGE that contain either mixed derivatives or are of quadratic order in φ, as these are expected to only contribute negligeable contributions to the dynamics in the vicinity of the critical point. This means effectively setting $\alpha = \kappa = 0$. As a result of these additional considerations, the dynamics of the Josephson phase in a realistic system are expected to be sufficiently described by

$$(\partial_x^2 - \partial_t^2 - \eta\partial_t)\varphi(x,t) - j_0(t)\sin\varphi(x,t) = \epsilon(x,t), \tag{3.43}$$

where the critical current $j_0(t)$ through the junction appears explicitly again.

3.2 Simulations

3.2.1 Preliminaries

Accompanying the experimental observations of defect formation, many numerical simulations have been performed in the field. Most of them could confirm the scaling exponents predicted by Z&K for large parts of the parameter space. However, apart from numerical anomalies which are usually attributed to finite-size effects, substantial deviations from scaling were observed that are assumed to extend Z&K qualitatively, supported by analytical approximations. Specifically for the three systems mentioned in the preceding chapter, Z&K suggests that the (inverse) correlation length – and thus the number of defects – should scale with the quenchtime via an

exponent $\sigma = 1/4$ (c.f. eqn. (2.38)). But in a number of publications a *doubling* of the exponent was proposed for large quenchtimes $\tau_q \gg \tau_0$. For such slow transitions, the number of defects becomes small and so we can alternative think about a putative doubling occurring for low defects densities, that is $\langle n^2 \rangle \ll 1$.

While for the $\mathbb{Z}_2$-type ionic crystals we derived the general behaviour in sec. 2.4 and found $\langle n^2 \rangle = \exp(-2L/\xi)$, for narrow (i.e. approximately $1d$) superconducting rings there also exists a proposition for the case of strong damping [16], and from the previous sections we assume this to be maintainable for $U(1)$-type ionic crystals. Different from the $\mathbb{Z}_2$ case above, we now have a continuous symmetry that is broken and instead of counting kinks, n now acts as a winding number as introduced in sec. 2.2. In contrast to the (anti-)kink density, the winding number density $n(x)$ varies continuously, as it simply corresponds to the phase gradient $\mathrm{d}\theta/\mathrm{d}x = n(x)$. Intuitively, if we assume fluctuations in $n(x)$ to be independent in space, we would replace the discrete Poisson distribution from the $\mathbb{Z}_2$ discussion by a Gaussian. And this is indeed what is found in [16], giving $\langle n(x)n(0) \rangle \simeq \exp(-x^2/2\xi^2)$ and thus $\langle n^2 \rangle \propto \exp(-[\tau_q/\tau_0]^2)$. In case of $L \gg \xi$, this leads to an estimate of $\langle n^2 \rangle \sim \mathcal{O}(L/\xi)$ – just as in the case of $\mathbb{Z}_2$. For $L \ll \xi$, the Jacobi Theta function has been used to render the Gaussian form periodic in L [31]. This yields an approximation of $\langle n^2 \rangle \propto \exp(-4\pi^2[\xi/L]^2)$, i.e. an *exponential damping* in the quenchtime instead of a scaling with the doubled exponent at large quenchtimes. But of course, the exponential form is not unlikely to be mistaken for doubling between two separated regimes.

For Joesphson junctions, the question how the defect density behaves for large τ_q is being complicated by an uncertainty about the temperature dependence of the critical current. In numerical simulations, linear dependence has shown $\sigma = 1/4$ while a quadratic dependence gave $\sigma = 1/2$ [32]. The relation between temperature and critical current is sensitive towards fabrication techniques and thus prevents a unique interpretation of experimental data so far.

Starting on this basis, the subsequently presented simulations were hoped to support these approximations and especially explore further the region of large τ_q. In addition, when simulating $\mathbb{Z}$-symmetry breaking in Josephson Junctions an attempt was made to gain some insights that have so far not been found in the literature.

3.2.2 Numerical approach

There are two types of differential equations that need to be considered. In the $U(1)$ case it is the Ginzburg-Landau (GL) type (3.39) (= (3.11)), which reduces to the correct equation for the $\mathbb{Z}_2$ breaking by considering a real instead of a complex field. The appropriate equation to simulate the $\mathbb{Z}$ breaking in long Josephson Junctions has been introduced as eqn. (3.43) and will be referred to as the JJ-type. All equations are evolved in time by using a modified leapfrog algorithm with a discretisation of $\Delta x = 0.2$ and $\Delta t = 0.05$, and so far only on *rings* of length $L = 32$, where – as in the following – dimensionless units are used. Exploring the effect of non-periodic boundary conditions and other lattice spacings and domain lengths is subject to future work.

In the GL-type cases, the temperature was maintained constant at $T = 0.01$ while

the phase transition was implemented by a *linear quench* of the form

$$\delta(t) = \begin{cases} -t/\tau_q & \text{for} \quad t \leq \tau_q \\ -1 & \text{for} \quad t > \tau_q \end{cases} . \tag{3.44}$$

and the evolution was performed from $t = -2\tau_q$ until the stationary state in which the defects were frozen out, which was the case at times $t \sim a\tau_q$ where $a \sim 1..10$ decreases with τ_q. The initial configuration of the fields is given by the unbroken equilibrium value, which is zero.

The evolution of the JJ-type equation is of slightly different nature. Here, the transition is implemented as a change in temperature in order to accommodate for different dependencies of the critical current. Hence, in [32] an exponential quench is suggested. However, as long as $\mathrm{d}T/\mathrm{d}t|_{t=0} = 1/\tau_q$ this is assumed to not alter significantly the expected number of defects [31]. Thus for our purposes it seemed preferable to implement a linear quench in T with the same form as eqn. (3.44) in order to arrange for better comparability of the results. The time interval of evolution was specified in the same way as described for the GL-cases. But now we are not evolving the order parameter but its phase. This must be assumed as being randomly distributed at the initial point in time, uniformly across the ring. That means however that we are not able to reflect true $\mathbb{Z}$-symmetry on the computer but rather need to constrain the initial phase to be distributed in a finite interval. It might then be interesting to explore in how far this *explicit* symmetry breaking in the initial configuration affects numerical results. It should be noted that once confined to a finite interval I, the phase will not leave I at any point during the transition and so different shapes of defects will form. In [32], scaling in accordance with the Z&K has been observed with good precision for small quenchtimes already when confining the initial phase to the interval $[0, 2\pi)$. The question of doubling however could not be answered completely. For the present simulations, a much weaker constraint was applied by assuming ϕ to be initially distributed across 100 intervals of 2π.

At the end of each evolution, the number defects n and its square could be read-off from the the final configuration. To obtain the ensemble average, this procedure had to be followed repeatedly. It was found that even in order to obtain acceptable qualitative results, the average had to be taken over $N \simeq 1500$ realisations. This meant a major practical hurdle. The available computing time was not enough to gather the desired amount results.

3.2.3 Results

The dependence of the final total density of kinks and antikinks is shown in fig. 3.2.3 for a statistical average over 2000 realisations. In the doubly logarithmic plot, the straight line for small quenchtimes confirms the prediction from Z&K. At large quenchtimes however, this gives way to a non-linear fall-off that corresponds to more than doubling in the slope. The linear appearance at large τ_q in the corresponding semi-logarithmic plot suggest exponential form. This would mean that exponential damping at small defect densities occurs not only in small superconducting rings but also in circular ion chains for which the transverse trapping potential is highly anisotropic.

While the result for $\mathbb{Z}_2$ should be expected to have considerable significance, the simulations of $U(1)$ and $\mathbb{Z}$ breaking could so far only be performed with averages over 100 realisations each. Nevertheless, a tendency should be possible to

extract. Fig. 3.2.3 shows plots of the average square number of defects $\langle n^2 \rangle$ versus the quenchtime τ_q. Large statistical variations are clearly visible at fast quenches already. At large quenchtimes however, the formation of defects becomes so unlikely that an average over only 100 realisations becomes completely unreliable, rather providing a lower bound. This is particularly true for the continuous $U(1)$ case. And indeed, the small-τ_q behaviour for $U(1)$ suggests $\sigma = 0.5$, in contradiction to the K&Z prediction. This aside, non-linear fall-off at small densities is indicated. The latter seems also present in the $\mathbb{Z}$ case. There, at small quenchtimes $\langle n^2 \rangle$ appears to scale with τ_q via an exponent different from 0.25 or 0.5. A linear fit over all points with $\tau_q < 10^3$ gave $\sigma = 0.38 \pm 0.035$ (with a 2σ confidence interval). Bearing in mind the low level of statistical significance, it is nevertheless tempting to interpret this as the mean between the values previously found for $\mathbb{Z}_2$ and $U(1)$ and thus confirming the intuitive picture of the discrete but finite group $\mathbb{Z}$ lying in between. A comparison to [32], where $\sigma = 0.25$ was found for the average number of defects $\langle |n| \rangle$, has so far not been made possible. To do this, the additional feature would be needed to extract the probability of finding only single kinks or antikinks. These numerical results are unsatisfying and will have to be tested and extended in the future. Apart from the need of accumulating more computing time, it will be necessary to implement the possibility of statistical error analysis.

While the quantitative results need to be improved, the qualitative behaviour of the system during the phase transitions could be observed without constraints, and figs. 3.2.3 – 3.2.3 provide some insights. As the system approaches the transition, fluctuations of the order parameter increase, giving rise to different choices between the new degenerate vacua at different positions in space. In an intermediate regime, fluctuation still allow to reverse some of these choices so that at the end only a small number of defects will have formed. Assuming a randomly distributed phase initially, the phase of the order parameter always condenses around the centre of its initial distribution. While the multiple kink-antikink structures that form while the $\mathbb{Z}$-breaking relax to simpler shapes until they freeze out, in the $U(1)$ case no intermediate stages have been observed in which the instantaneous winding number exceeded 1.

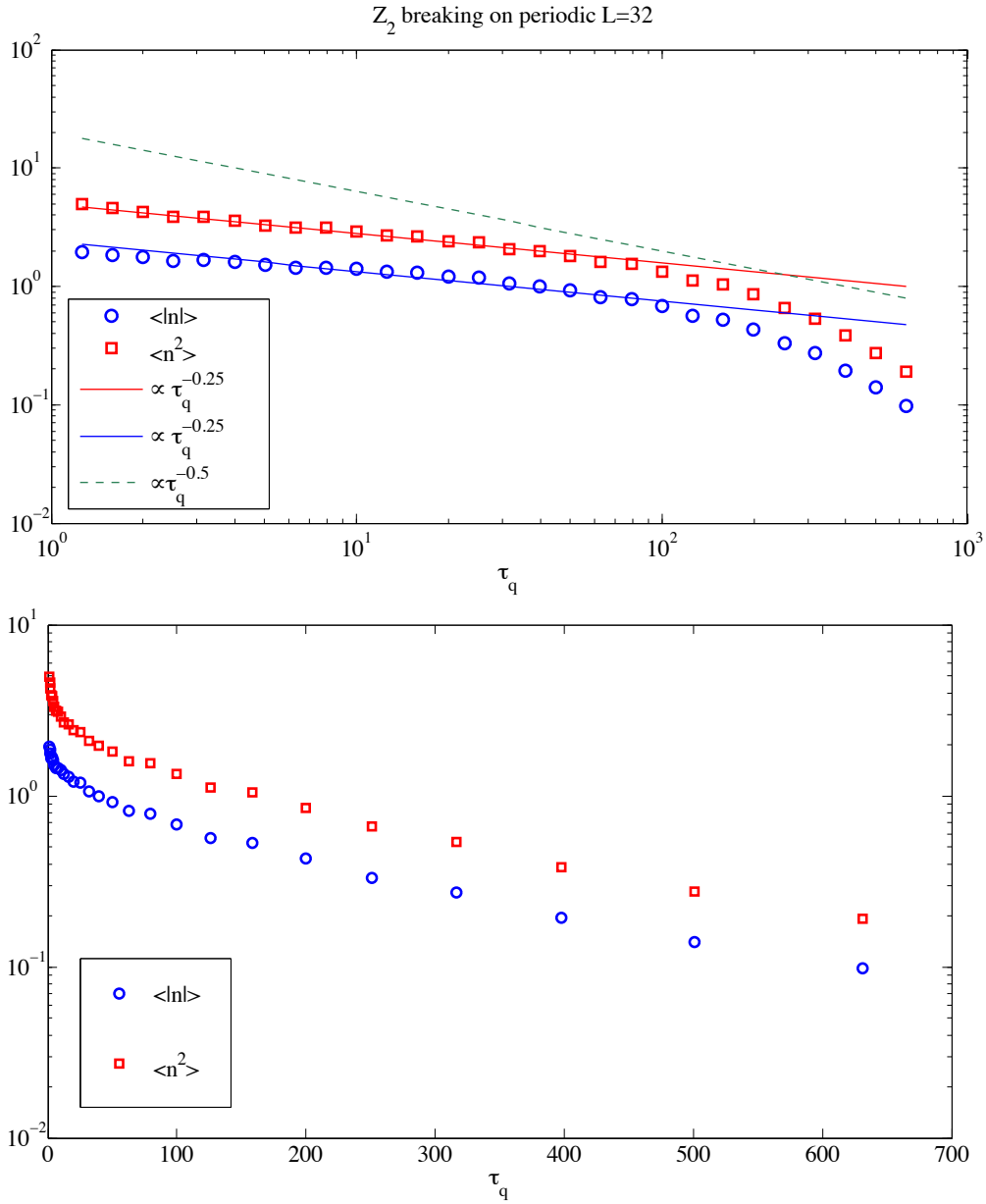

Figure 3.2: Dependence of the expected number $\langle|n|\rangle$ and squared number $\langle n^2\rangle$ of (kinks+antikinks) on the quenchtime τ_q for periodic boundary conditions. At small quenchtimes ($\tau_q \lesssim 10^2$), the Z&K scaling prediction with $\sigma = 0.25$ is observed. When τ_q gets larger, defect densities become smaller and the exponential damping in τ_q becomes perceivable. This can clearly be distinguished from a mere doubling in σ and is consistent with the linear appearance at large τ_q in the semilogarithmic plot.

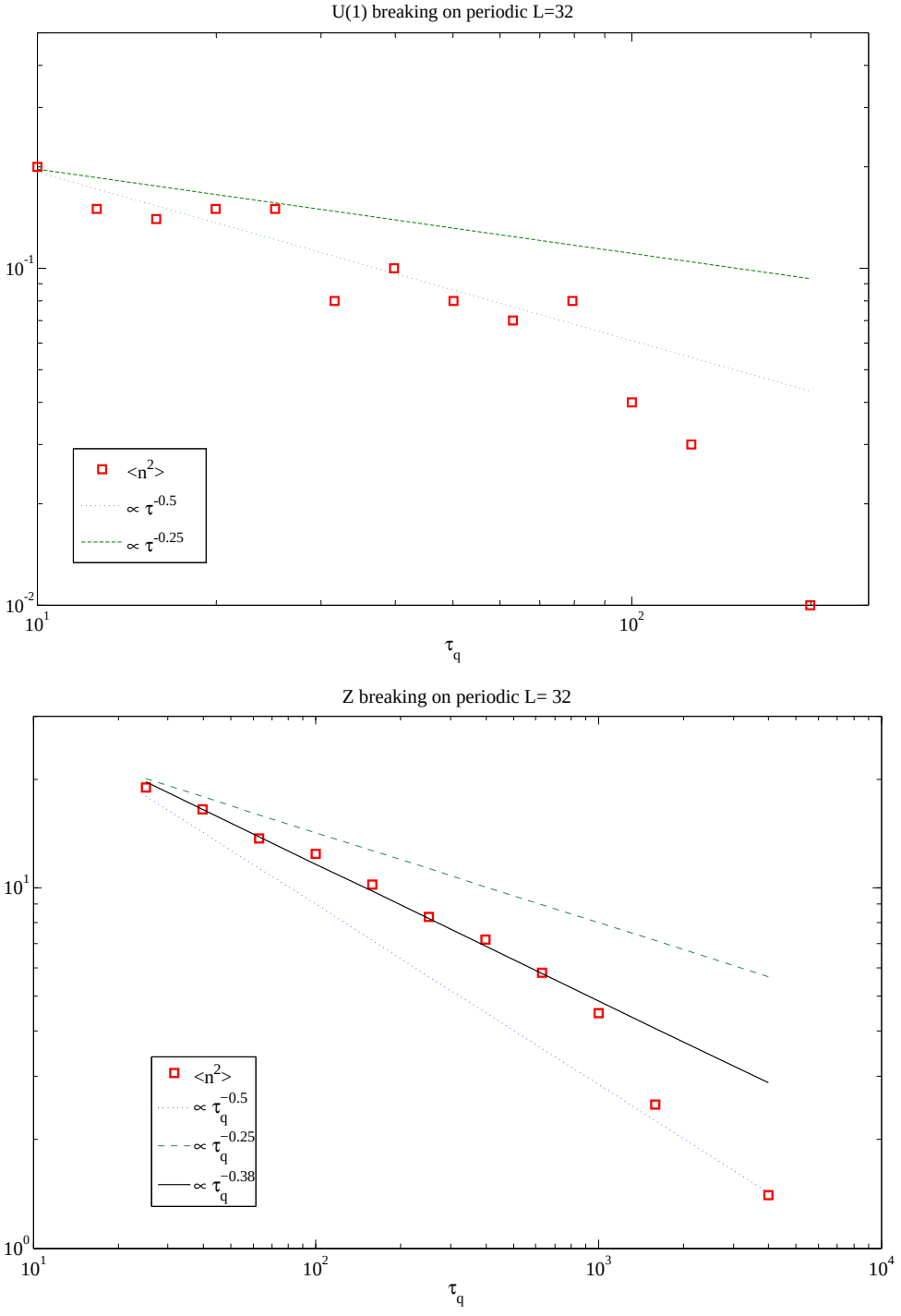

Figure 3.3: Average square number of defects $\langle n^2 \rangle$ versus quenchtime τ_q for periodic boundary conditions in the cases of strongly damped $U(1)$-breaking (*top*) and $\mathbb{Z}$-breaking (*bottom*) at low temperatures. The statistical average could only be taken over 100 realisations.

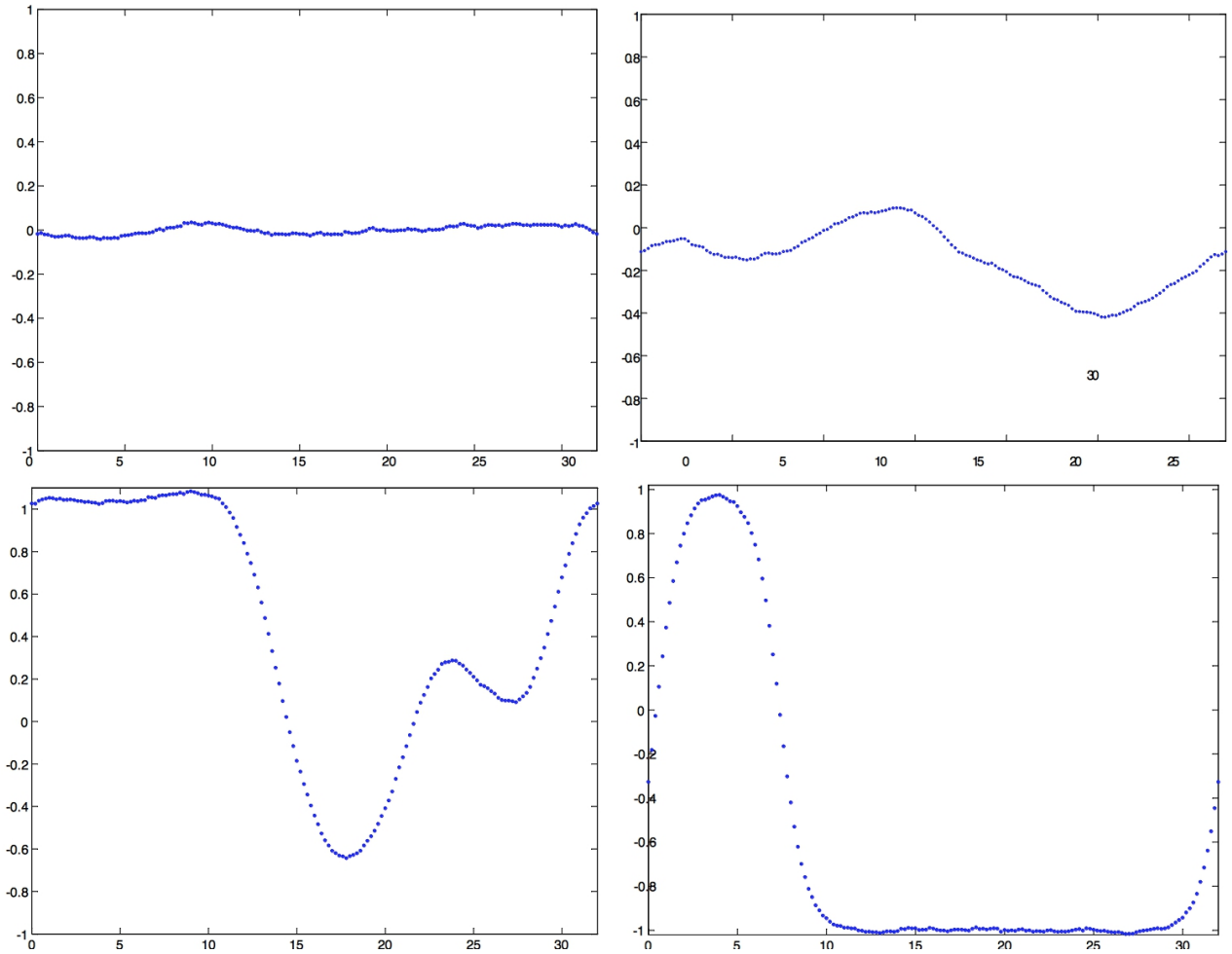

Figure 3.4: Different stages of the evolution of the order parameter Φ during representative realisations of a $\mathbb{Z}_2$-breaking phase transition. Increasing time from left to right and top to bottom. Horizontal axes correspond to space, while the vertical axes give the value Φ.

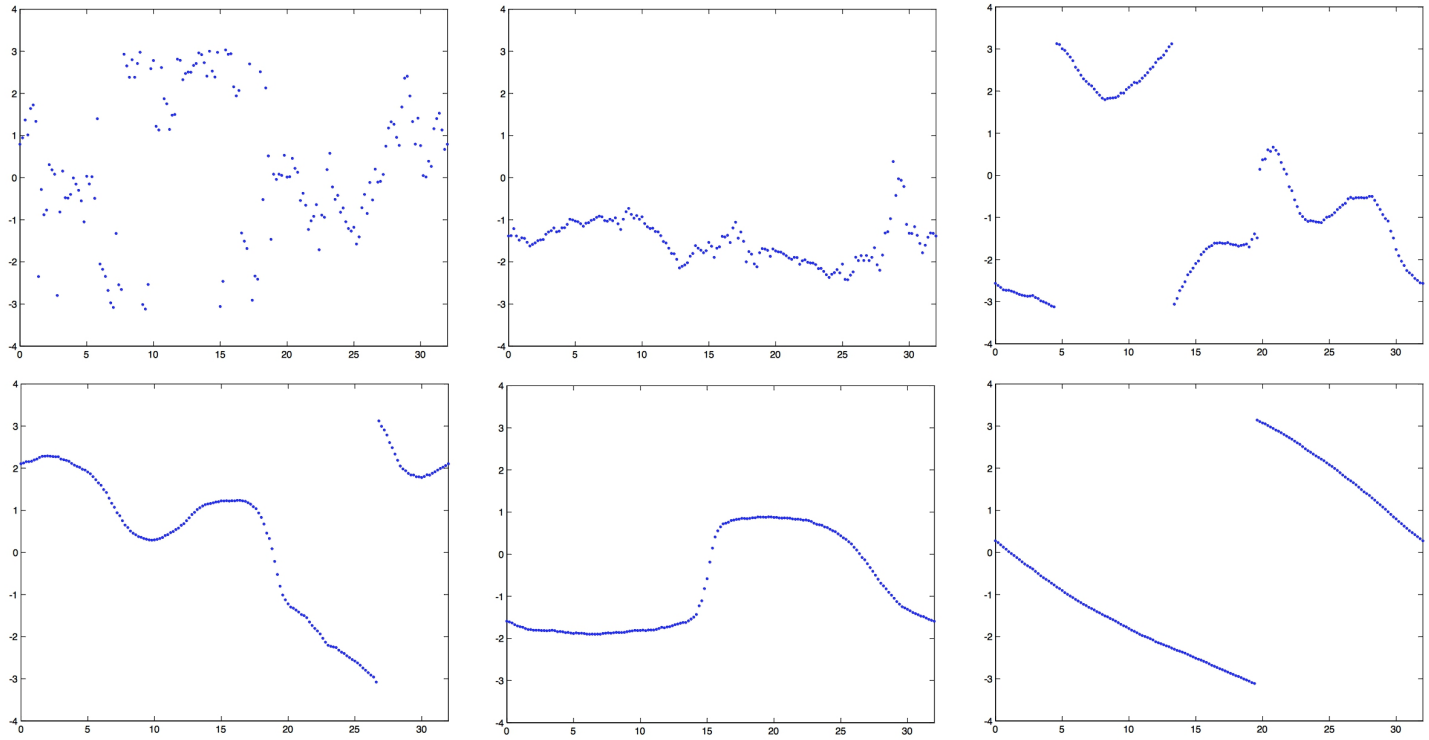

Figure 3.5: Different stages of the evolution of the order parameter phase θ during representative realisations of a $U(1)$-breaking phase transition. Increasing time from left to right and top to bottom. Horizontal axes correspond to space, while the vertical axes give the value of θ.

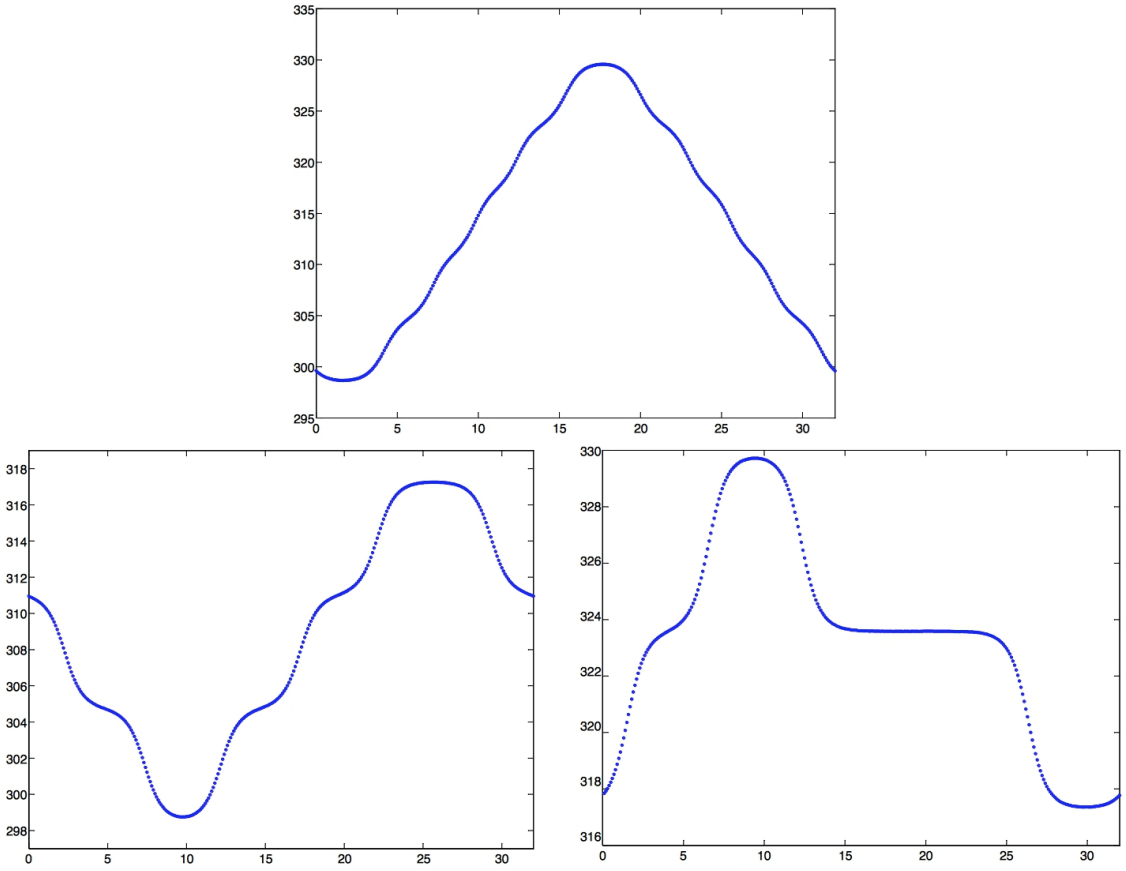

Figure 3.6: Different stages of the evolution of the order parameter phase θ during representative realisations of a $\mathbb{Z}$-breaking phase transition. Increasing time from left to right and top to bottom. Horizontal axes correspond to space, while the vertical axes give the value of θ.

Summary & Outlook

This work explained the basic principles that are responsible for the existence of phase transitions and the production of defects. In particular, we saw how the behaviour of systems near a critical point can be understood in terms of a number of scale-invariant laws and how this gives rise to a division of different kinds of systems into only a few universal classes. The fundamental reason for this could be identified as the divergence of correlations at the critical point and the idea of renormalisation was introduced as a way to understand critical behaviour as a flow in the landscape of theories. Importantly, we saw how the loss of symmetry in the realisations of a system during a continuous phase transitions leads to the production of defects when causality introduces bounds on the correlations within a system and we elucidated how the shape of those defects coming from the breaking of a continuous symmetry can completely be determined in topological terms. It has also been explained how the Kibble-Zurek mechanism uses the scaling assumption from the equilibrium dynamics to estimate defect densities. Although the success of this approach has been realised for many situations, we could see how finite-size effects in condensed matter can lead to a departure form scaling. Specifically for low defect densities the proposal of an exponential suppression of defect production with increasing quenchtime was discussed and supported by numerical analysis.

Among all possible systems, three have been chosen to be discussed in more detail and exemplify the preceding general concepts. Each of them represents one of the smallest possible symmetry groups of its kind. Ionic crystals, depending on the exact experimental realisation have been shown to be suitable for the study of spontaneous breaking of either the finite symmetry group $\mathbb{Z}_2$ or the continuous $U(1)$. The latter has also been seen realisable in annular superconductors. Spontaneous breaking of the discrete but infinite symmetry group $\mathbb{Z}$ was found to happen in Josephson Junction that are cooled down across the superconducting phase transition. While in the $\mathbb{Z}_2$ case the defects are primitive kinks, $\mathbb{Z}$ breaking causes the formation of defects that can be characterised as compound kinks. $U(1)$ breaking leads to flux trapping as it is predicted by its topological classification.

Due to limited computed time available, the numerical work is far from complete and significant quantitative results could not be established. It is intended to support the few performed simulations by further runs which explore the behaviour at different domain lengths, other quench forms and other values of damping. It would also be necessary to see the results for non-periodic boundary conditions. Also, an account an account of other observables like the probabilities to find a certain number of defects would be of virtue.

So far however, strong indication has been found for the expected scaling regime

at small quenchtimes is present for all three symmetries. In particular, the Kibble-Zurek prediction was found in the $\mathbb{Z}_2$ case with statistical significance. For all three symmetries, a non-linear fall-off at large quenchtimes is evident and could be attributed to finite-size effects at low defect densities. For $\mathbb{Z}_2$ this fall-off appeared to have exponential form as it was proposed already for $U(1)$.

Acknowledgements

Foremost, I would like to express my deep gratitude towards Ray Rivers, who introduced me to a topic that left me with great fascination. Working on this dissertation became a pleasure under his kind supervision.

I would also like to thank David Weir, without whom I would most likely have missed the experience to peek into the interior of phase transitions.

Thanks also to all those who made this last year possible. And to those who made it joyful.

Bibliography

[1] Wojciech H. Zurek. The shards of broken symmetry. *Nature*, 382:1175–1204, Jul 1996.

[2] Nigel Goldenfeld. *Lectures on phase transitions and the renormalization group*. Frontiers in Physics, 1992.

[3] *Fundamental of Statistical and Thermal Physics*.

[4] J. Fröhlich and T. Spencer. The phase transition in the one-dimensional ising model with 1/r2 interaction energy. *Commun. Math. Phys.*, 84(87), 1982.

[5] F. Baroni. The mechanism of phase transitions of infinite-range systems enlightened by an elementary Z_2 symmetric classical spin model. (arXiv:1106.3870), 2013.

[6] Crystal statistics. i. a two-dimensional model with an order-disorder transition.

[7] Igor Herbut. *A Modern Approach to Critical Phenomena*. Cambridge UP, 2007.

[8] E. A. Guggenheim. The principle of corresponding states. *Journal of Chemical Physics*, 13:253, 1945.

[9] Scaling laws for ising models near t_c.

[10] Michel le Bellac, Fabrice Mortessagne, and G. George Batrouni. *Equilibrium and Non-Equilibrium Statistical Thermodynamics*. Cambridge UP, 2004.

[11] Maurice Kléman. The topological classification of defects. In *Formation and Interactions of Topological Defects*, volume 349 of *NATO ASI Series*. Plenum Press, 1995.

[12] T.W.B. Kibble. Some implications of a cosmological phase transition. *Physics Reports*, 67(1):183 – 199, 1980.

[13] T. W. B. Kibble. Phase transitions in the early universe and defect formation. In *Formation and Interactions of Topological Defects*, volume 349 of *NATO ASI Series*. Plenum Press, 1995.

[14] W. H. Zurek. Cosmological experiments in condensed matter systems. *Physics Reports*, 276:177–221, 1996.

[15] G. Karra and Ray J. Rivers. The densities, correlations and length distributions of vortices produced at a gaussian quench. *arXiv*, (9603413v1), 2012.

[16] David J. Weir and Ray J. Rivers. Fluxoid formation: size effects and non-equilibrium universality. *arXiv*, 2011.

[17] *Ion Traps*.

[18] Daniel H. E. Dubin and T. M. O'Neil. Trapped nonneutral plasmas, liquids, and crystals (the thermal equilibrium states). *Rev. Mod. Phys.*, 71:87–172, Jan 1999.

[19] J. P. Schiffer. Phase transitions in anisotropically confined ionic crystals. *Phys. Rev. Lett.*, 70:818–821, Feb 1993.

[20] S. Ulm, J. Roßnagel, et al. Observation of kibble-zurek scaling law for defect formation in ion crystals. *Nature Communications*, 4(2290), 2013.

[21] C. Champenois, M. Marciante, J. Pedregosa-Gutierrez, M. Houssin, M. Knoop, and M. Kajita. Ion ring in a linear multipole trap for optical frequency metrology. *Phys. Rev. A*, 81:043410, Apr 2010.

[22] K. Okada, K. Yasuda, et al. Crystallization of ca^+ ions in a linear rf octupole ion trap. *Phys. Rev. A*, 75:033409, Mar 2007.

[23] G. Birkl, S. Kassner, et al. Multiple-shell structures of laser-cooled 24mg+ ions in a quadrupole storage ring. *Nature*, 357:310–13, 1992.

[24] T. Schatz, U. Schramm, and D. Habs. Multiple-shell structures of laser-cooled 24mg+ ions in a quadrupole storage ring. *Nature*, 412:717–20, 2001.

[25] R. Nigmatullin, A. del Campo, G. De Chiara, G. Morigi, M.B. Plenio, and A. Retzker. Formation of helical ion chains. *arXiv*, (1112.1305v1), 2011.

[26] Shmuel Fishman, Gabriele De Chiara, Tommaso Calarco, and Givanna Morigi. Structural phase transition in low-dimensional ion crystals. *Physical Review B*, 77(064111), 2008.

[27] J. Bardeen, L. N. Cooper, and J. R. Schrieffer. Theory of superconductivity. *Phys. Rev.*, 108:1175–1204, Dec 1957.

[28] Sergio Pagano. *Nonlinear dynamics in long Josephson junctions*. PhD thesis, The Technical University of Denmark, 1987.

[29] R. P. Feynman, R. B. Leighton, and M. Sands. The schrödinger equation in a classical context: a seminar on superconductivity. In *The Feynman Lectures on Physics*, volume 3, chapter 21. Addison-Wesley, 1965.

[30] A. Barone and G. Paterno. *Physics and Applications of the Josephson Effect*. John Wiley and Sons, 1982.

[31] Ray J. Rivers. *Personal communication*.

[32] Anna V. Gordeeva and Andrey L. Pankratov. Defect formation in long josephson junctions. *Phys. Rev. B*, 81:212504, Jun 2010.